

1  
2  
3  
4  
5  
6  
7  
8  
9  
10  
11  
12  
13  
14  
15  
16  
17  
18  
19  
20  
21  
22  
23  
24  
25  
26  
27  
28  
29  
30  
31  
32  
33  
34  
35  
36  
37  
38  
39  
40  
41  
42  
43  
44  
45  
46  
47  
48  
49  
50

**Evolution of circadian behavioral plasticity through *cis*-regulatory divergence of a neuropeptide gene**

Michael P. Shahandeh<sup>1,\*</sup>, Liliane Abuin<sup>1</sup>, Lou Lescuyer De Decker<sup>1</sup>, Julien Cergneux<sup>1</sup>, Rafael Koch<sup>2</sup>, Emi Nagoshi<sup>2</sup> and Richard Benton<sup>1,\*</sup>

<sup>1</sup>Center for Integrative Genomics  
Faculty of Biology and Medicine  
University of Lausanne  
CH-1015  
Lausanne  
Switzerland

<sup>2</sup>Department of Genetics and Evolution &  
Institute of Genetics and Genomics of Geneva (iGE3)  
University of Geneva  
CH-1205  
Geneva  
Switzerland

\*Corresponding authors:  
[michaelparviz.shahandeh@unil.ch](mailto:michaelparviz.shahandeh@unil.ch)  
[Richard.Benton@unil.ch](mailto:Richard.Benton@unil.ch)

51 **Abstract**

52

53 Widely-distributed species experience substantial environmental variation, which  
54 they often accommodate through behavioral plasticity. Although this ability is  
55 integral to fitness, we have little understanding of the mechanistic basis by which  
56 plasticity evolves. One factor that varies seasonally and by latitude is photoperiod  
57 (day length). Many organisms, including the cosmopolitan *Drosophila*  
58 *melanogaster* display circadian plasticity, adjusting to fluctuating photoperiod by  
59 varying the timing of their activity to coincide with changing dawn/dusk intervals<sup>1</sup>.  
60 Here, we compare *D. melanogaster* with the closely-related ecological specialist  
61 *Drosophila sechellia*, an equatorial island endemic that experiences minimal  
62 photoperiod variation, to investigate the molecular-genetic basis of circadian  
63 plasticity evolution<sup>2,3</sup>. We discover that *D. sechellia* displays exceptionally little  
64 circadian plasticity compared to *D. melanogaster* and other non-equatorial  
65 drosophilids. Through a screen of circadian mutants in *D. melanogaster/D.*  
66 *sechellia* hybrids, we identify a role of the neuropeptide Pigment-dispersing factor  
67 (Pdf) in this loss. While the coding sequence of *Pdf* is conserved, we show that *Pdf*  
68 has undergone *cis*-regulatory divergence in these drosophilids. We document  
69 species-specific temporal dynamic properties of *Pdf* RNA and protein expression,  
70 as well as Pdf neuron morphological plasticity, and demonstrate that modulating  
71 Pdf expression in *D. melanogaster* can influence the degree of behavioral plasticity.  
72 Furthermore, we find that the *Pdf* regulatory region exhibits signals of selection  
73 across populations of *D. melanogaster* from different latitudes. Finally, we provide  
74 evidence that plasticity confers a selective advantage for *D. melanogaster* at higher  
75 latitudes, while *D. sechellia* likely suffers fitness costs through reduced copulation  
76 success outside its range. Our work defines *Pdf* as a locus of evolution for circadian  
77 plasticity, which might have contributed to both *D. melanogaster's* global  
78 distribution and *D. sechellia's* habitat specialization. Moreover, together with spatial  
79 changes in Pdf expression reported in high-latitude drosophilid species<sup>4,5</sup>, our  
80 findings highlight this neuropeptide gene as a hotspot for circadian plasticity  
81 evolution.

82

83 **Introduction**

84

85 Nervous systems coordinate animals' behavioral responses to the external world  
86 to maximize survival and fitness. This task becomes more challenging when  
87 environments are not constant, a problem of substantial significance for broadly-  
88 distributed species. One way to face changing conditions is with behavioral  
89 plasticity, that is, the ability to adjust behavioral phenotypes to match fluctuations  
90 in the environment. There are many examples of plastic behaviors in nature:  
91 songbirds shift the frequency of their vocalizations in response to anthropogenic  
92 noise<sup>6</sup>, ants alter their locomotor and foraging behaviors as a function of  
93 temperature<sup>7</sup>, and lizards change their basking behavior based on altitude<sup>8</sup>.  
94 However, we have little understanding of whether and how behavioral plasticity is  
95 determined and evolves at the genetic and cellular level.

96

97 An important example of plastic behavior in animals is circadian activity,  
98 whereby species adjust their daily activity patterns in response to seasonal  
99 variation in day length<sup>9</sup>. This ability is critical because circadian activity in most  
100 animals coordinates specific behaviors with optimal activity periods throughout the  
day to, for example, avoid environmental stressors, maximize food availability, and

101 align with conspecifics for synchronized social and sexual behaviors<sup>10,11</sup>. As such,  
102 deviations from regular circadian patterns can negatively affect fitness and species  
103 persistence<sup>12,13</sup>. *Drosophilids* are a powerful system to study circadian behavioral  
104 plasticity. These flies display large bouts of activity surrounding dawn and dusk  
105 (termed morning and evening activity peaks), separated by a period of relative  
106 inactivity during the middle of the day<sup>14</sup>. The best-studied species, the  
107 cosmopolitan *Drosophila melanogaster*, plasticly adjusts its circadian rhythm  
108 depending upon seasonal variation in photoperiod<sup>1</sup>. Notably, the degree of  
109 photoperiod plasticity of different strains of this species correlates with the latitude  
110 of collection site<sup>15</sup>. Moreover, several distantly-related, high-latitude species have  
111 evolved divergent patterns of activity and extreme plasticity, allowing their daily  
112 activity to match long summer days<sup>16</sup>.

113 A potentially interesting comparison species to *D. melanogaster* is  
114 *Drosophila sechellia*, a much closer relative that diverged 3-5 million years ago  
115 (Fig. 1a)<sup>2,3</sup>. *D. sechellia* is endemic to the equatorial islands of the Seychelles  
116 archipelago, where it experiences almost no seasonal photoperiod variation (Fig.  
117 1a-b). Here, we discover striking differences in the circadian activity and plasticity  
118 of *D. sechellia* and *D. melanogaster*, notably an almost complete inability of *D.*  
119 *sechellia* to adapt to increased photoperiod. Taking advantage of the possibility to  
120 interbreed these species, we conducted a genetic screen of known circadian  
121 genes, offering unprecedented insights into the genetic and cellular underpinnings  
122 of circadian plasticity evolution, and a rare connection between genetic divergence  
123 and evolved differences in an ecologically-relevant behavior.

124

## 125 Results

126

### 127 ***D. sechellia* displays reduced photoperiod plasticity compared to *D.*** 128 ***melanogaster***

129

130 To test for species-specific differences in circadian plasticity, we first measured  
131 circadian behavior for *D. melanogaster* and *D. sechellia* under a standard 12 h  
132 light-dark cycle (12:12 h LD) as well as four extended photoperiod regimes ranging  
133 from mild (14:10 h LD) to extreme (20:4 h LD) (Fig. 1c). We used males of two  
134 strains each of *D. melanogaster* and *D. sechellia* (Supplementary Table 1), to  
135 distinguish interspecific from intraspecific phenotypic differences. The two *D.*  
136 *melanogaster* strains (*DmelCS* and *DmelOR*) were collected at ~41° N and ~44°  
137 N, respectively, while the *D. sechellia* strains (*Dsec07* and *Dsec28*) are from the  
138 Seychelles archipelago, at ~4° S of the equator (Fig. 1a). The strains of each  
139 species therefore initially evolved in environments where they experienced large  
140 differences in annual photoperiod variation (Fig. 1b). Under each photoperiod, all  
141 strains displayed activity peaks during the morning and evening, although the  
142 timing of the evening peak varied by photoperiod (Fig. 1c). We quantified for each  
143 fly the average evening peak time of the last 4 of 7 days in a given photoperiod,  
144 allowing the first 3 days to serve as an acclimation period (Fig. 1c). For both *D.*  
145 *melanogaster* strains, we observed that as photoperiod increases, the timing of the  
146 evening activity peak is commensurately delayed (Fig. 1c). By contrast, for our *D.*  
147 *sechellia* strains, we observed strikingly little photoperiod plasticity, with a median  
148 delay in evening peak time of maximum ~1 h regardless of photoperiod length (Fig.  
149 1c). Additionally, under all photoperiod regimes, *D. sechellia* ended its afternoon

150 siesta and began ramping up to evening peak activity a few hours earlier than *D.*  
151 *melanogaster* (Fig. 1c).

152

153 ***D. sechellia* displays reduced morning peak activity compared to *D.***  
154 ***melanogaster***

155

156 We noted that *D. sechellia* is far less active during the dark phase than either *D.*  
157 *melanogaster* strain and displays little, if any, morning anticipation, i.e., increasing  
158 activity in the hours leading up to lights-on (Fig. 1c-d). Quantification of pre-dawn  
159 activity under 12:12 h LD in the 3 h preceding lights-on revealed prominent  
160 differences between the species (Fig. 1d): *D. sechellia* is generally very inactive  
161 during this time period, while the *D. melanogaster* strains display ample, albeit  
162 strain-specific, activity. These observations led us to question whether the morning  
163 peak of *D. sechellia* is a true activity peak or merely a startle response to lights-on.  
164 To address this issue, we measured free-running activity by acclimating our strains  
165 to 12:12 h LD before submitting them to constant dark conditions (DD). Both *D.*  
166 *melanogaster* and *D. sechellia* remained rhythmic under DD (Fig. 1e), and each  
167 strain displayed a period of ~24 h (Extended Data Fig. 1). By contrast, while *D.*  
168 *melanogaster* displayed clear activity peaks at the subjective dawn, *D. sechellia*  
169 exhibited very little activity at this timepoint, even during the first day of DD (Fig.  
170 1e). This result supports the hypothesis that the morning peak of *D. sechellia*  
171 observed under LD conditions (Fig. 1c) is predominantly a startle response to  
172 lights-on. Consistently, when we quantify morning peak timing under 12:12 h LD,  
173 we found that *D. melanogaster* reached peak activity before lights-on, as previously  
174 described<sup>17</sup>, while *D. sechellia* peaked only at or after lights-on (Fig. 1f).

175

176 **Reduced circadian plasticity and morning activity represent an evolutionary**  
177 **loss in *D. sechellia***

178

179 To determine if the species differences in circadian plasticity and morning activity  
180 represent an evolutionary loss in *D. sechellia* or a trait gain in *D. melanogaster*, we  
181 measured the activity of additional *D. melanogaster* strains collected from the  
182 Lower Zambezi Valley (close to its ancestral range<sup>18</sup> (~16° S), as well as strains of  
183 two species that have a more recent common ancestor with *D. sechellia* (Fig. 1a):  
184 *D. simulans* (collected from Madagascar, its ancestral range<sup>19</sup>, ~19° S) and *D.*  
185 *mauritiana* (a species endemic to Mauritius, ~20° S) (Extended Data Fig. 2a).  
186 Comparing 12:12 h and 16:8 h LD conditions, we observed a similar larger degree  
187 of circadian plasticity (~2 h evening peak delay under the longer photoperiod) for  
188 all of these strains compared to *D. sechellia* (~1 h evening peak delay). All of these  
189 strains also exhibited significant morning anticipation (Extended Data Fig. 2b).  
190 These results indicate that the lack of plasticity and reduction in morning peak  
191 activity observed in *D. sechellia* likely represent evolutionary losses in this lineage,  
192 and point to a potential connection between these two phenotypes.

193

194 **A genetic screen for differences in circadian activity and plasticity**

195

196 To identify the mechanistic basis of the species differences in circadian behaviors,  
197 we employed a candidate genetic screening approach. Extensive research in *D.*  
198 *melanogaster* has defined central brain circuitry of 150 circadian neurons, divided  
199 into discrete groups with differing effects on circadian activity and network

200 dynamics<sup>20</sup>. Within each neuron, a gene regulatory feedback loop allows each cell  
201 to track a ~24 h period<sup>21-23</sup> and to control the rhythmic expression of downstream  
202 effector genes (Fig. 2a). The members of this network serve as excellent  
203 candidates for explaining species-specific circadian behaviors. To take as  
204 unbiased an approach as possible, we obtained loss-of-function mutations for the  
205 majority of the genes encoding proteins within this feedback loop in addition to  
206 several in the downstream network, including the neuropeptide Pigment-dispersing  
207 factor (Pdf), as well as other circadian neuropeptides, CCHA1 and ITP  
208 (Supplementary Table 1). Our cross-species behavioral analyses (Fig. 1c-d and  
209 Extended Data Fig. 2) indicated that reduced circadian plasticity and morning peak  
210 activity in *D. sechellia* represent evolutionary losses. We therefore reasoned that  
211 the causal *D. sechellia* alleles were more likely to be recessive to *D. melanogaster*,  
212 and designed a screen in *D. melanogaster*-*D. sechellia* hybrids (Fig. 2b). In brief,  
213 we generated hemizygous test hybrids containing *D. melanogaster* mutants for  
214 each individual candidate gene, to reveal the recessive phenotype of the *D.*  
215 *sechellia* allele at the same locus. We also generated heterozygous control hybrids,  
216 using the *D. melanogaster* *w*<sup>1118</sup> strain (the most common genetic background of  
217 our mutant strains) or CS<sup>W</sup> strain (in the case of *Pdf*; see Methods) and each of our  
218 *D. sechellia* strains. These control hybrids have one allele each from *D.*  
219 *melanogaster* and *D. sechellia*. Thus, any differences we observe between control  
220 and test hybrids is likely due to the loss of the *D. melanogaster* allele in the test  
221 hybrid background. To control for genetic background effects<sup>24</sup>, we tested hybrids  
222 of both the *Dsec07* and *Dsec28* backgrounds. Finally, gene dosage effects were  
223 assessed by testing control hemizygotes in a (non-hybrid) *D. melanogaster*  
224 background, i.e., mutants crossed to *w*<sup>1118</sup> or CS<sup>W</sup>. Genes whose mutations  
225 displayed an effect in both test hybrid backgrounds compared to control hybrids,  
226 and no effect in hemizygous *D. melanogaster*, were considered the strongest  
227 candidates explaining interspecific phenotypic differences (Fig. 2c).

228

### 229 **The *Pigment-dispersing factor* gene underlies evolved differences in** 230 **circadian plasticity**

231

232 To assess candidate genes for an effect on circadian plasticity, we observed test  
233 and control hybrids under a 16:8 h LD photoperiod. Control hybrids of either the  
234 *w*<sup>1118</sup> (Extended Data Fig. 3a-d) or CS<sup>W</sup> background (Fig. 2d-e) display a larger  
235 degree of phenotypic plasticity than their *D. sechellia* parental strain, confirming  
236 that the *D. melanogaster* genotype underlying plasticity is at least partially dominant  
237 to that of *D. sechellia*, though the degree of dominance depends on the *D.*  
238 *melanogaster* parental strain. We screened 14 genes covering the majority of the  
239 circadian transcriptional feedback loop and many of its modulator and effector  
240 genes. Mutations in only one reduced circadian plasticity in both test hybrid  
241 backgrounds but not in hemizygous *D. melanogaster*: *Pdf* (Fig. 2d-e, Extended  
242 Data Fig. 3e-f). This is a promising gene for explaining species differences  
243 because, in *D. melanogaster*, Pdf is essential for delaying the phase of the  
244 endogenous clock circadian neurons under long photoperiods<sup>25</sup>, and flies lacking  
245 Pdf expression display reduced plasticity<sup>26,27</sup>.

246

247

248

249 **Potential broad-scale divergence of the circadian clock underlies *D.***  
250 ***sechellia*'s reduced morning peak activity**

251

252 We also screened these genotypes under 12:12 h LD and quantified pre-dawn  
253 activity (Extended Data Fig. 4a-d). In contrast to the dominance of the *D.*  
254 *melanogaster* phenotype for circadian plasticity (Extended Data Fig. 3a-d), *w*<sup>1118</sup>  
255 control hybrids display intermediate pre-dawn activity relative to either parental  
256 strain, suggesting a more complex genetic architecture of this species difference.  
257 Consistent with this idea, four genes displayed an effect in test hybrids of both  
258 backgrounds (Fig. 2f-g) and not in hemizygous *D. melanogaster* flies (Extended  
259 Data Fig. 4e-g). These encode the core transcriptional feedback loop protein CYC  
260 and the light-sensitive CRY, which is responsible for light-dependent  
261 synchronization of the molecular clock<sup>28-30</sup>, as well as Hr38 and VRI, which are  
262 neural activity-dependent transcriptional or post-transcriptional regulators of *Pdf*  
263 expression, respectively<sup>31</sup>.

264

265 ***Cis*-regulatory evolution of *Pdf***

266

267 We subsequently focused our attention on *Pdf*, because of its unique significant  
268 effect on circadian plasticity and evidence that *trans*-regulation of *Pdf* expression  
269 influences morning peak activity. To understand how this gene differs between  
270 species, we first compared the *Pdf* coding sequence of 10 *D. melanogaster* and 6  
271 *D. sechellia* isogenic strains (as well as 5 *D. simulans* lines). These sequences are  
272 predicted to encode peptides of near-perfect conservation, with no species-specific  
273 differences (Extended Data Fig. 5).

274 We therefore reasoned that divergence between species must be due to  
275 expression differences of *Pdf*. In *D. melanogaster*, this neuropeptide is expressed  
276 exclusively in 8 neurons in each central brain hemisphere: 4 large ventrolateral  
277 clock neurons (l-LNvs), which represent a subset of the “evening” cells, and 4 small  
278 ventrolateral clock neurons (s-LNvs), the “morning” cells (Fig. 3a). These neuronal  
279 subtypes have predominant roles in controlling evening and morning activity,  
280 respectively<sup>32-34</sup>, although a functional clock is required in both for photoperiod  
281 plasticity<sup>33,35</sup>. Through qualitative *Pdf* immunofluorescence analysis, we observed  
282 a conserved spatial pattern of *Pdf* expression in *D. sechellia* (Fig. 3b), consistent  
283 with a survey of *Pdf* expression across a broader range of drosophilids<sup>36</sup>. This result  
284 suggested that species-specific differences instead exist in the temporal pattern  
285 and/or levels of expression.

286 Because our hybrid screen identified an effect of the *Pdf* locus itself, we  
287 hypothesized that differences in expression must result from divergence in the *cis*-  
288 regulatory region. To test this possibility, we cloned ~2.4 kb of genomic DNA  
289 immediately 5' of the start codon of *Pdf* from either *D. melanogaster* or *D. sechellia*  
290 – based upon a previous analysis in *D. melanogaster*<sup>37</sup> – upstream of a GFP  
291 reporter gene<sup>38</sup>. These transgenes were integrated in an identical genomic location  
292 in the same *D. melanogaster* genetic background, thereby permitting comparison  
293 of their activity in a common *trans* and genomic environment. As expected, both  
294 species' *Pdf* reporters exclusively labelled the l-LNvs and s-LNvs (Fig. 3c). We first  
295 measured reporter expression in the l-LNvs because, in *D. melanogaster*, *Pdf*  
296 expression in these cells is required to plasticly adjust the timing of the evening  
297 peak<sup>4</sup>. To process all samples in parallel for quantitative comparisons, we focused  
298 on behaviorally relevant time points under 12:12 h LD and 16:8 h LD conditions

299 (Fig. 3d-e). In the I-LNVs, throughout the evening activity peak under both  
300 photoperiods, the *D. sechellia* 5'-regulatory region consistently drives lower and  
301 more constant reporter expression relative to the *D. melanogaster* sequence (Fig.  
302 3d-e). Notably, the *D. melanogaster Pdf* reporter displayed a sudden drop in  
303 expression at 8 h (under 12:12 h LD) or at 12 h (under 16:8 h LD), prior to returning  
304 to a higher level, which potentially reflects a new pulse in transcriptional activity  
305 that appears sensitive to photoperiod.

306 In *D. melanogaster*, the s-LNVs are essential for resetting the phase of the  
307 circadian clock (likely through the cyclic release of Pdf<sup>39,40</sup>) and are necessary for  
308 morning peak activity<sup>32,34</sup>. We therefore compared reporter expression in the s-LNV  
309 axonal projections – where the largest cyclic Pdf expression is observed over a 24  
310 h period<sup>37</sup> – for four time points spanning the morning activity peak (Fig. 3f). We  
311 again observed that the *D. sechellia* sequence drives lower expression of the  
312 reporter but, in contrast to the I-LNVs during the evening peak, with a similar  
313 temporal fluctuation in expression. Together these results confirm functional  
314 divergence of the 5' cis-regulatory region between *D. sechellia* and *D.*  
315 *melanogaster*. This sequence is most likely to affect transcriptional activity but,  
316 because it encompasses the 5'-UTR of *Pdf*, we cannot exclude that it (also)  
317 influences transcript stability and/or translatability<sup>41</sup>.

318

### 319 **Modifying *Pdf* expression reduces the magnitude of circadian plasticity and** 320 **morning anticipation**

321

322 Having identified species-specific properties in the cis-regulatory element of *Pdf*,  
323 we tested whether these would be sufficient to impact behavior. Taking advantage  
324 of the different reporter expression levels driven by the *D. melanogaster* and *D.*  
325 *sechellia Pdf* 5' regions (Fig. 3d-f), we used these same sequences to generate  
326 Pdf neuron Gal4 drivers to induce “strong” (*D. melanogaster Pdf-Gal4*) or “weak”  
327 (*D. sechellia Pdf-Gal4*) knock-down of *Pdf* using a *UAS-Pdf<sup>fRNAi</sup>* effector<sup>42</sup>. We first  
328 validated the anticipated distinct efficacy of RNAi with quantitative single molecule  
329 RNA fluorescence *in situ* hybridization (smFISH). In *DmelPdf-Gal4>Pdf* RNAi flies,  
330 *Pdf* transcripts were reduced to ~4% of the levels of control animals, while *DsecPdf-*  
331 *Gal4>Pdf* RNAi flies expressed *Pdf* transcripts at ~20% of control levels (Extended  
332 Data Fig. 6).

333 We first observed these flies under 16:8 h LD conditions and quantified  
334 evening peak timing (Fig. 3g-h). The *DmelPdf-Gal4>Pdf* RNAi flies displayed a  
335 dramatic reduction in evening peak time relative to controls. By contrast, *DsecPdf-*  
336 *Gal4>Pdf* RNAi flies display a small, and non-significant, decrease in evening peak  
337 time relative to control animals, with a notable increase in variance. Importantly,  
338 there is a significant difference between the RNAi-expressing genotypes despite  
339 their otherwise identical genetic backgrounds. We also observed the behavior of  
340 these flies under 12:12 h LD, and quantified pre-dawn activity (Fig. 3i-j). Both  
341 *DmelPdf-Gal4>Pdf* RNAi and *DsecPdf-Gal4>Pdf* RNAi flies have reduced pre-  
342 dawn activity relative to controls. However, the *DmelPdf-Gal4>Pdf* RNAi flies  
343 displayed significantly less pre-dawn activity than the *DsecPdf-Gal4>Pdf* RNAi  
344 flies. Together these results indicate that the level (and possibly temporal  
345 dynamics) of *Pdf* expression – as determined by species-specific 5' cis-regulatory  
346 regions – is sufficient to affect both circadian plasticity and morning anticipation in  
347 an otherwise identical genetic background.

348

### 349 **Species-specific, photoperiod-dependent differences in *Pdf* RNA expression**

350

351 We next investigated how *cis*-regulatory divergence might influence endogenous  
352 *Pdf* RNA and protein expression. Using smFISH, we compared *Pdf* transcript levels  
353 between *D. melanogaster* and *D. sechellia* at the same fine temporal resolution as  
354 for the transgenic reporters. Under 12:12 h LD, quantification of transcript levels in  
355 I-LNvs throughout the evening peak revealed slightly higher initial *Pdf* expression  
356 in *D. sechellia* than *D. melanogaster* (Fig. 4a). The most striking difference,  
357 however, is a sudden drop in *Pdf* transcripts in *D. melanogaster*, but not *D.*  
358 *sechellia*, after lights-off (Fig. 4a). Under 16:8 h LD conditions, this reduction in *Pdf*  
359 RNA levels is no longer present (Fig. 4b). These observations indicate that  
360 transcriptional activity of *Pdf* is more dynamic in *D. melanogaster* than *D. sechellia*,  
361 resulting in a decrease of *Pdf* transcripts by the dark phase under 12:12 h LD. Such  
362 a pattern might additionally/alternatively result from differences in RNA stability  
363 between species. Regardless of the mechanism, this species-specific transcript  
364 depletion appears sensitive to photoperiod. Interestingly, such a pattern of *Pdf*  
365 transcription in the I-LNvs has not been previously described using bulk or single-  
366 cell RNA sequencing of these neurons in *D. melanogaster*<sup>43,44</sup> when sampling more  
367 broadly across a 24 h time period; however a decrease in *Pdf* RNA at 14 h (relative  
368 to the 2 h time point) was previously documented using smFISH<sup>45</sup>, congruent with  
369 our results.

370 When we quantified *Pdf* RNA in the s-LNvs throughout the morning activity  
371 peak, we found that *Dmel*CS displayed overall more *Pdf* RNA than *Dsec07* at each  
372 time point, particularly in the pre-dawn time points, with *Dsec07* reaching near-  
373 similar levels only after lights-on (Fig. 4c). This difference in *Pdf* RNA levels is  
374 concordant with the differences in pre-dawn activity we observed between these  
375 species (Fig. 1c-d), and the implication of transcriptional and post-transcriptional  
376 regulators of *Pdf* expression in species-specific morning anticipation (Fig. 2f-g).

377

### 378 **Species- and photoperiod-dependent differences in *Pdf* protein expression**

379

380 We next used immunofluorescence to compare *Pdf* protein expression in *D.*  
381 *melanogaster* and *D. sechellia*. Similar to the transcript analyses, we quantified *Pdf*  
382 immunofluorescence in the I-LNvs in time points surrounding the evening activity  
383 peak under 12:12 h LD and 16:8 h LD conditions (Extended Data Fig. 7a-b). Under  
384 both photoperiods, we observed qualitative differences between these species in  
385 the overall pattern of staining intensity, but the much greater variability in signal  
386 intensity of these samples, particularly for *D. sechellia* under 16:8 h LD, made it  
387 difficult to connect back to our more quantitative measures of *Pdf* RNA levels (or to  
388 behavioral activity).

389 In the s-LNvs, we quantified *Pdf* fluorescence in the axonal projections for  
390 the same time points spanning the morning activity peak (Fig. 4d). In the relatively  
391 short time window analyzed, we observed a consistently high level of *Pdf* in *D.*  
392 *melanogaster*, including in the hours preceding lights-on. By contrast, in *D.*  
393 *sechellia*, *Pdf* signal is lower in the pre-dawn hours, and increases to an equivalent  
394 amount as *D. melanogaster* only by lights-on. This pattern corresponds well to that  
395 of the relative levels of *Pdf* transcripts, and to species differences in pre-dawn  
396 activity at these times (Fig. 1c-d). We also analyzed *Pdf* immunofluorescence in  
397 the s-LNv cell bodies, which display higher and less cyclic *Pdf* expression in *D.*  
398 *melanogaster*<sup>37</sup>. Consistently, we found *Pdf* signal remains high across the morning

399 peak times in the s-LNV soma of *D. melanogaster* (Fig. 4e). In *D. sechellia*, the Pdf  
400 signal begins high and drops significantly only after lights-on (Fig. 4e). Together,  
401 our observations of Pdf RNA levels and Pdf protein levels/distribution in the s-LNVs  
402 of *D. sechellia* suggest that this species has a smaller and/or shorter pulse of Pdf  
403 expression around the morning peak compared to *D. melanogaster*, such that once  
404 this neuropeptide accumulates to high levels in the axon terminals at/after lights-  
405 on (Fig. 4d), it becomes depleted in the soma (Fig. 4e). Species-specific dynamics  
406 in Pdf spatial distribution might also reflect differences in intracellular transport  
407 and/or secretion pathways.

408

### 409 **Species-specific circadian structural plasticity of Pdf neurons**

410

411 In *D. melanogaster*, the axonal projections of the s-LNVs to the dorsal circadian  
412 neurons (Fig. 3a) display circadian structural plasticity, reaching peak branching  
413 complexity during the day, and lower complexity during the night<sup>46</sup>. This  
414 phenomenon depends, at least in part, on cyclic expression and release of Pdf from  
415 both the s-LNVs and l-LNVs and the expression of the Pdf receptor<sup>42</sup>. To test if the  
416 observed species-specific temporal patterns of Pdf expression are accompanied  
417 by differences in the remodeling of these neurons, we quantified the branching  
418 complexity of s-LNV projections in *D. melanogaster* and *D. sechellia* during the light  
419 (2 h) and dark (14 h) phases (Fig. 4f). During the light phase, we found statistically  
420 indistinguishable levels of complexity in the two species. However, in *D.*  
421 *melanogaster*, branching complexity is significantly lower in the dark phase when  
422 compared to *D. sechellia* (Fig. 4f). This apparent reduction of structural plasticity of  
423 *D. sechellia* Pdf neurons corroborates the less dynamic changes in Pdf expression  
424 in this species.

425

### 426 **Signals of cis-regulatory evolution and selection on the Pdf regulatory region**

427

428 Having characterized functional divergence of the Pdf cis-regulatory region  
429 between species, we next asked whether the *D. sechellia* sequence exhibits any  
430 evolutionary signature. We sequenced this region in all of our *D. melanogaster*, *D.*  
431 *sechellia* and *D. simulans* strains. Overall, *D. simulans* and *D. melanogaster*  
432 sequences share an average of ~97% pairwise sequence similarity, while *D.*  
433 *sechellia* has an average pairwise sequence similarity of ~93% with *D.*  
434 *melanogaster*. We used these sequences to construct a maximum likelihood  
435 phylogeny (Fig. 5a). In contrast to the species tree, the Pdf 5'-regulatory  
436 sequences from *D. sechellia* form a monophyletic group, while the *D. melanogaster*  
437 and *D. simulans* sequences mostly cluster together (with the exception of a single  
438 *D. simulans* sequence, which groups more basally with the *D. sechellia*  
439 sequences). Motif enrichment analysis<sup>47</sup> identified putative regulatory sequences  
440 in these species' 5' regions. While all such motifs were shared among the *D.*  
441 *melanogaster* and *D. simulans* sequences, 8 of these sites are degenerated or  
442 absent in *D. sechellia* (and one site is unique to this species) (Fig. 5b), indicating  
443 that sequence divergence in the *D. sechellia* Pdf regulatory region is likely to affect  
444 its function activity, potentially through the loss of transcription factor binding sites.

445

446 We next investigated whether the sequence divergence between *D.*  
447 *melanogaster* and *D. sechellia* 5'-regulatory sequences might result, at least in part,  
448 from natural selection on variants underlying circadian plasticity at higher latitudes.  
We examined this possibility by determining whether variants within the *D.*

449 *melanogaster Pdf* 5'-regulatory region are associated with higher degrees of  
450 circadian plasticity observed with increasing latitudes<sup>15</sup>. The reverse analysis in *D.*  
451 *sechellia* is not possible as this species is restricted to an equatorial latitude. Taking  
452 advantage of a dataset of single nucleotide variant frequencies in the genomes of  
453 globally-distributed populations of *D. melanogaster*<sup>48</sup>, we chose 13 populations  
454 representing a wide range of latitudes (Fig. 5c); all had a minimum read-depth of 5  
455 to ensure confidence in variant frequencies. We calculated the average minor allele  
456 frequency (MAF) across all variable sites detected within the *Pdf* 5'-regulatory  
457 sequence and plotted these against the estimated latitude of the population  
458 collection site. Because correlations could reflect the underlying population  
459 structure as a result of demographic history as *D. melanogaster* emigrated from its  
460 native range in Africa<sup>49</sup>, as a control, we repeated this analysis for the putative  
461 equivalent regulatory region (2.4 kb upstream from the start codon) of six other  
462 neuropeptide genes. We found a strong positive correlation (Spearman's rho =  
463 0.77) between population latitude and MAF for the *Pdf* 5'-regulatory region, but not  
464 for any of the other neuropeptide genes (Fig. 5c, Extended Data Fig. 8). These  
465 comparisons indicate that the effect of latitude on MAF of the *Pdf* 5'-regulatory  
466 sequence is different than we would expect due to demography alone, suggesting  
467 a potential role for selection on these sites in *D. melanogaster*. These results are  
468 similar to recent reports of clinal variation in other circadian genes<sup>50-53</sup>.

469 Lastly, we checked the MAFs of these variable sites in our laboratory strains.  
470 These single nucleotide variants occur with a MAF of ~25% among our *D.*  
471 *melanogaster* strains, but none were present in any of our *D. sechellia* strains (Fig.  
472 5d). These results are consistent with a potential function of these variants in  
473 increasing circadian plasticity. Together with the predicted motif differences  
474 between *D. melanogaster* and *D. sechellia Pdf* 5'-regulatory sequences (Fig. 5b),  
475 these data will help guide future analyses of the specific functional changes within  
476 this region.

477

## 478 **Circadian plasticity is important for reproductive success**

479

480 To identify a mechanism by which natural selection might act, we asked if plasticity  
481 in circadian activity impacts fitness. Photoperiod has been shown to affect lifespan  
482 in many insects and other animals<sup>54-56</sup>, leading us to reason that if flies have  
483 reduced lifespans under extended photoperiod, then this might lead to reduced  
484 total reproductive output. We recorded survivorship of individual *D. melanogaster*  
485 and *D. sechellia* maintained at either 12:12 h or 16:8 h LD (Fig. 5e). Flies of both  
486 species maintained under 16:8 h LD displayed a significant reduction in lifespan  
487 relative to those under 12:12 h LD. This result is surprising in that it suggests that  
488 *D. melanogaster's* ability to plasticly adjust its activity to longer days does not  
489 alleviate the cost of exposure to longer photoperiod. However, the detrimental  
490 effect of longer photoperiod was not observed until after several weeks in both  
491 species, in which time flies could certainly mate and produce offspring. It is  
492 therefore unclear if the effect of extended photoperiod on lifespan would impact  
493 fitness in nature, where lifespan is likely much shorter than under laboratory  
494 conditions.

495

496 Circadian rhythms are important for synchronizing sexual behavior among  
497 conspecifics<sup>10,11</sup>. We therefore reasoned that if circadian plasticity (or the lack  
498 thereof) impacted copulation success, it would likely impact fitness. To test this  
possibility, we acclimated male and female *D. melanogaster* and *D. sechellia*

499 virgins to 12:12 h LD and 16:8 h LD for 4 days. We then observed copulation rates  
500 among male-female pairs in two assays: first, over a 2-hour period just after lights-  
501 on (Fig. 5f), and second, over the course of one week (Fig. 5g). For *D.*  
502 *melanogaster*, we observed no difference in copulation rates of flies between  
503 treatments in either experiment. By contrast, there was a significant decrease in  
504 copulation by *D. sechellia* acclimated to 16:8 h LD. Specifically, the decrease in  
505 copulation rate in the short-term assay was largely maintained over the course of  
506 several days in our long-term assay, indicating that flies that did not copulate within  
507 2 h were unlikely to do so several days later. These results demonstrate that *D.*  
508 *sechellia*'s reproductive output – and thus fitness – is highly likely to be impacted  
509 by its lack of circadian plasticity under extended photoperiods that it would never  
510 normally experience in nature. These data also suggest that by plasticly adjusting  
511 its behavior, *D. melanogaster* is able to circumvent these negative effects.

512

## 513 Discussion

514

515 Identifying the genetic and neural mechanisms of behavioral plasticity is key to  
516 understanding how organisms evolve(d) to inhabit variable environments, as well  
517 as to projecting how they will persist in increasingly unstable ones<sup>57</sup>. However,  
518 efforts to uncover the proximate causes of behavioral divergence are limited by a  
519 lack of genetic access to multiple closely-related species, leaving remarkably few  
520 cases where the molecular and/or cellular underpinnings of interspecific  
521 differences in behaviors have been mapped<sup>58</sup>, with the vast majority being in  
522 (peripheral) sensory pathways (e.g.,<sup>59-63</sup>). Here, we have uncovered molecular and  
523 cellular mechanisms of circadian plasticity differences in drosophilids, providing a  
524 rare example linking differences in gene function, central neuron populations, and  
525 behavioral differences between species.

526 By comparing the equatorial *D. sechellia* with closely-related, globally-  
527 distributed species, we discovered a dramatic difference in the degree of  
528 photoperiod plasticity and provided evidence for a key contribution of the *cis*-  
529 regulatory region of the *Pdf* locus in this difference (Fig. 5h). In *D. melanogaster*,  
530 *Pdf* expression is required in the l-LNVs for photoperiod plasticity<sup>27</sup>, and previous  
531 comparative work has described interspecific spatial differences in *Pdf*  
532 expression<sup>36</sup>, notably in high-latitude species where *Pdf* is restricted to the l-  
533 LNVs<sup>4,16</sup>. Importantly, prior to our work, no functional connection between  
534 divergence at the *Pdf* locus and species differences in behavior had been  
535 established. Nevertheless, these observations, combined with our analyses in *D.*  
536 *sechellia* and *D. melanogaster* – including the evidence for latitude-based selection  
537 on the *D. melanogaster Pdf5'*-regulatory region – point to the *Pdf* locus as a hotspot  
538 of evolution. Given *Pdf*'s terminal placement as an effector gene of the clock  
539 network<sup>31</sup>, its role in broadly synchronizing circadian clock neurons<sup>64</sup>, and its strong  
540 impact on circadian behaviors, changes in the *cis*-regulation of *Pdf* expression  
541 might represent a minimally pleiotropic means of introducing plasticity into the clock  
542 neuronal network, akin to regulatory changes of developmental genes that underlie  
543 morphological evolution<sup>65</sup>. By contrast, divergence of core clock genes might  
544 represent a more complex evolutionary trajectory, necessitating the coevolution of  
545 multiple interacting loci.

546 *Pdf* evidently does not explain the entirety of the species differences in  
547 plasticity: there are almost certainly contributions of additional loci that we have not  
548 tested and/or more complex genetic interactions that we cannot identify with our

549 screen design. For example, the possibility of transvection (*trans*-regulation of  
550 alleles on homologous chromosomes)<sup>24</sup> in our hybrid screen might have masked  
551 the contributions of some divergent loci. Our observation of differences between  
552 *Pdf cis*-regulatory activity using transcriptional reporters, and endogenous *Pdf* RNA  
553 and Pdf protein levels in *D. sechellia* and *D. melanogaster* suggest that additional  
554 genes might nevertheless ultimately impact Pdf. Beyond species-specific *cis*-  
555 regulation characterized here, post-transcriptional regulation of *Pdf*<sup>31</sup>, as well as  
556 control of the transport and secretion of this neuropeptide<sup>66</sup> are also potentially  
557 subject to divergent regulation. Indeed, in *D. melanogaster*, a *D. virilis*  
558 transcriptional reporter for *Pdf* labels the s-LNvs (in addition to several non-  
559 circadian cells) despite this species, like other high-latitude drosophilids<sup>4,16</sup>, lacking  
560 endogenous Pdf expression in these neurons<sup>5</sup>; these observations suggest that  
561 mechanisms other than (or in addition to) *cis*-regulatory divergence underlie this  
562 spatial difference in expression. Finally, molecules functioning downstream of Pdf  
563 in controlling plasticity (e.g., Eyes absent<sup>67</sup>) are possible loci of evolutionary  
564 adaptations.

565 *D. sechellia* also displays greatly reduced morning activity compared to  
566 other drosophilids. As this phenotype is similar to that observed in *D. melanogaster*  
567 *Pdf* mutants<sup>68</sup>, it is perhaps surprising that we did not find an effect of the *Pdf* locus  
568 itself in this difference. Rather, we identified several genes with the ability to  
569 regulate *Pdf* expression in *trans*, highlighting a different evolutionary trajectory to  
570 divergence of circadian plasticity that nevertheless converges upon this  
571 neuropeptide. The morning and evening oscillators partially overlap in function,  
572 sharing synaptic feedback<sup>27,69</sup>, with both being required for long photoperiod  
573 adaptation<sup>35</sup>. The mechanistic and evolutionary connection (if any) between  
574 divergence of circadian plasticity and morning activity warrants further exploration.  
575 The reason, if any, for reduced morning peak activity in *D. sechellia* remains  
576 unclear; this issue might be illuminated by future analysis of the circadian pattern  
577 of other aspects of this species' behavior, such as courtship or feeding.

578 *D. sechellia*'s loss of photoperiod plasticity is particularly intriguing in the  
579 context of this species' specialist ecology for the noni fruit of *Morinda citrifolia*, on  
580 which it exclusively feeds and breeds. Niche specialization has involved substantial  
581 evolution of its chemosensory behaviors<sup>59,70-75</sup>. Our work extends knowledge of this  
582 species' phenotypic divergence to non-host related behaviors. Why loss of  
583 circadian plasticity of *D. sechellia* likely leads to a severe fitness cost at high  
584 latitudes is unknown, but we speculate that longer photoperiods result in altered  
585 pheromone production, as observed in different seasonal morphs of *Drosophila*  
586 *suzukii*<sup>76</sup>. A more general consideration is why *D. sechellia* has lost circadian  
587 plasticity. One hypothesis is that in a constant environment, selection to maintain  
588 plasticity mechanisms is relaxed, leading them to degenerate over time.  
589 Alternatively, in stable environments, plasticity might come at a fitness cost, leading  
590 selection to favor its loss under constant conditions to enhance, for example, the  
591 robustness of this species' circadian activity. While we cannot currently  
592 discriminate between these two possibilities, if the latter is correct, our view of *D.*  
593 *sechellia*'s specialization must expand beyond host fruit preference evolution to  
594 restriction to an equatorial environment. Indeed, *D. sechellia*'s circadian phenotype  
595 might contribute to its restriction to the Seychelles archipelago, despite the much  
596 larger modern range of *M. citrifolia*<sup>77</sup>. Exploration of the impact of differences in  
597 circadian plasticity mechanisms to latitudinal constraint of other species seems  
598 warranted.

599

## 600 **Acknowledgements**

601

602 We are grateful to Enrico Bertolini, Charlotte Förster, Daniel Matute, Julia Saltz, the  
603 Bloomington *Drosophila* Stock Center (NIH P40OD018537) and the  
604 Developmental Studies Hybridoma Bank (NICHD of the NIH, University of Iowa)  
605 for reagents. We thank Roman Arguello, Enrico Bertolini, David Gatfield and  
606 members of the Benton laboratory for discussions and comments on the  
607 manuscript. Research in E.N.'s laboratory is supported by the SNSF  
608 (310030\_189169), and R.B.'s laboratory is supported by the University of  
609 Lausanne, an ERC Advanced Grant (833548) and the SNSF (310030B\_185377).

610

## 611 **Author Contributions**

612

613 M.P.S. and R.B. conceived the project. M.P.S. designed, performed and analyzed  
614 most experiments. L.A. performed the hybrid screening and sequencing of the *Pdf*  
615 gene region. L.L.D.D. contributed to the experiments in Fig. 1c. J.C. contributed to  
616 the experiments in Extended Data Fig. 3 and 4. R.K. assisted with preliminary  
617 behavioral experiments and, together with E.N. and R.B., provided input on  
618 experimental design, analysis and interpretation. M.P.S. and R.B. wrote the paper  
619 with feedback from all other authors.

620

## 621 **Competing interests**

622

623 The authors declare no competing interests.

624

625

## 626 **Methods**

627

### 628 ***Drosophila* strains and rearing**

629

630 All flies were reared on a wheat flour-yeast-fruit juice media in non-overlapping 2-  
631 week cycles kept in 12:12 h LD at 25°C. For *D. sechellia* strains, we added an  
632 additional mixture of instant *Drosophila* medium (Formula 4-24 blue, Carolina bio-  
633 supply) mixed with juice of their host noni fruit (Raab Vitalfood).

634 For behavioral comparisons of *D. melanogaster*, *D. sechellia*, *D. simulans*,  
635 and *D. mauritiana* circadian behavior, at least two wild-type strains of each species  
636 were used (*DmelCS*, *DmelOR*, *DmelLZV L72*, *DmelLZV L76*, *Dsec07*, *Dsec28*,  
637 *DsimMD221*, *DsimMD242*, *Dmau90*, and *Dmau91*). To screen candidate genes for  
638 effects on differences in circadian behavior between *D. melanogaster* and *D.*  
639 *sechellia*, we used *D. melanogaster* strains containing known loss-of-function  
640 mutations for genes previously associated with circadian behavior in *D.*  
641 *melanogaster*. A list of all fly strains and their hybridization success (when  
642 applicable), is provided in Supplementary Table 1. When strains were not available  
643 (*vriille*) or not hybridizable (*Jet* and *timeless*), we used *D. melanogaster* deficiency  
644 strains, containing engineered chromosomal deletions spanning the region of a  
645 candidate gene, in addition to many other loci<sup>79</sup>. In the case of *timeless*, a  
646 deficiency strain did not hybridize either. The *Pdf* strain we used is the *pdf<sup>01</sup>* allele<sup>68</sup>  
647 in the Canton-S genetic background (provided by Charlotte Förster), as we were  
648 unable to hybridize the original *pdf<sup>01</sup>* strain. To confirm that the effect we found  
649 (Extended Data Fig. 3) was not due to a difference in *D. melanogaster* genetic  
650 background, we additionally compared it to the same parental Canton-S (denoted  
651 here *DmelCS<sup>W</sup>*, where “W” = Würzburg), which displayed qualitatively similar pre-  
652 dawn activity and circadian plasticity to our own *DmelCS* strain (Extended Data  
653 Fig. 9).

654

### 655 **Hybrid crosses and circadian candidate gene screening**

656

657 To screen available circadian candidate genes, we created *D. melanogaster/D.*  
658 *sechellia* hybrids as previously described<sup>80</sup>. In brief, very young virgin females were  
659 crossed to males that were collected as virgins and aged in high density for 5-7  
660 days. To increase their interactions, we pushed a plug into the vial to leave 2-3 cm  
661 height above the food surface. These crosses yield only sterile but viable males.  
662 This method does not allow us to test sex-linked candidate genes, such as the core  
663 transcriptional feedback loop member *period<sup>81</sup>*, and the Pdf receptor gene, *Pdfr<sup>64</sup>*.  
664 We aimed to phenotype at least 15 hybrids of each genotype, but due to the strong  
665 reproductive isolation between species, some genotypes were difficult to cross to  
666 *D. sechellia*, resulting in a low sample size.

667

### 668 ***Drosophila* activity monitoring**

669

670 For all activity monitoring, we used 1-3 day old males in the *Drosophila* activity  
671 monitor (DAM) system<sup>82</sup> stored in small incubators that continuously monitor light  
672 and temperature conditions (TriTech Research DT2-CIRC-TK). In brief, this system  
673 uses an infrared beam that bisects a 5 mm glass tube, in which the fly is stored, to  
674 record activity as the number of beam crosses per minute. Flies are stored in tubes  
675 with a 5% sucrose 2% agar w/v solution at one end, and capped with a cotton plug

676 at the other. Each monitor records the activity of up to 32 flies simultaneously, and  
677 multiple monitors are stored in a single incubator. For each genotype, we recorded  
678 flies over at least two technical replicates.

679 All flies were first exposed to 7 days of 12:12 h LD, and then shifted to one  
680 of four extended photoperiod cycles for an additional 7 days: 14:10, 16:8, 18:6, or  
681 20:4 h LD to allow us to measure 12:12 h LD-associated (i.e., morning anticipation)  
682 and extended photoperiod-associated behaviors (i.e., evening peak plasticity) for  
683 each fly. For assessment of free-running period, flies were exposed to 7 days of  
684 DD following 7 days of 12:12 h LD. For each photoperiod regime, we took the  
685 average activity of the final 4 days of each week-long period. The initial 3 days were  
686 considered an acclimation period, and were discarded. All subsequent analyses  
687 were performed in R using the Rethomics package<sup>83</sup>.

688 To quantify pre-dawn activity, the average normalized activity was  
689 calculated for each fly in 30 min bins in the 3 h preceding dawn. To quantify morning  
690 and evening peak times, peak activity was identified from the average activity of  
691 each fly in 10 min bins during the last 4 days of both the 12:12 h LD and extended  
692 photoperiod using custom R scripts (available at:  
693 [github.com/mshahandeh/circ\\_plasticity](https://github.com/mshahandeh/circ_plasticity)). First, a rolling triangular mean was  
694 applied to smooth the data. The data was split into two 12 h sections, the first  
695 spanning the time around lights-on and the second spanning the time around lights-  
696 off (at least 3 h preceding and 3 h after for both). The global peak was identified  
697 within each data set and recorded as the timing of the morning peak and evening  
698 peak, respectively.

699

## 700 **Construction of transgenic lines**

701

702 ~2.4 kb upstream of the *Pdf* start codon was PCR amplified from *D. melanogaster*  
703 (*DmelCS*) or *D. sechellia* (*Dsec28*) genomic DNA and Gateway cloned into the  
704 pDONR221 vector, sequenced-verified, and subcloned into both pHemmarG  
705 (Addgene #31221) for CD4:tdGFP reporters, and pBPGUw (Addgene #17575) for  
706 Gal4 drivers. Constructs were injected and integrated into the attP2 landing site  
707 (chromosome 3) in the *D. melanogaster* genome by BestGene Inc.  
708 Oligonucleotides used for cloning and sequence verification are listed in  
709 Supplementary Table 3.

710

## 711 **Single molecule mRNA FISH**

712

713 We performed single molecule mRNA fluorescent in-situ hybridization to quantify  
714 *pdf* mRNA expression at various time points in the s-LNvs and l-LNvs. We used  
715 the *Pdf* probe library described previously<sup>45</sup> bound to the Cy5 fluorophore  
716 (LubioScience), and adapted a published protocol<sup>84</sup>. Brains were imaged using an  
717 inverted confocal microscope (Zeiss LSM 710 or 880) equipped with a 40× or 63×  
718 oil immersion objective using fixed settings to maximize comparability of images  
719 within experiments. Images were processed in Fiji and RNA spots were counted  
720 using the Fiji macro RS-FISH<sup>85</sup>. No signal was detected outside of the LNv cell  
721 bodies. We compared RNA spot counts between strains within photoperiod  
722 treatments using a Wilcoxon rank-sum test followed by post-hoc correction for  
723 multiple tests<sup>86</sup>. We did not compare between experiments as these flies were  
724 dissected, stained and imaged separately. We repeated smFISH throughout the  
725 morning peak to ensure replicability of the overall pattern of expression. We did not

726 pool these data as they are from a separate staining/imaging and may not be as  
727 comparable.

728

## 729 **Immunofluorescence**

730

731 For immunofluorescence of whole-mount *Drosophila* brains, 1-2 day old males  
732 were collected and acclimated to a specific photoperiod for 4 additional days. To  
733 standardize sampling times, we fixed these flies in 4% paraformaldehyde for 2 h at  
734 room temperature with gentle agitation prior to dissection. Brains were dissected  
735 and stained essentially as described<sup>87</sup>. Primary and secondary antibodies and  
736 concentrations used are provided in Supplementary Table 2. Brains were imaged  
737 using an inverted confocal microscope (Zeiss LSM 710 or 880) equipped with a  
738 20× or 40× objective using fixed settings to maximize comparability of images. To  
739 quantify fluorescence, images were processed in Fiji, by first creating a maximum  
740 intensity projection Z-stack which was then thresholded to remove background  
741 signal<sup>88</sup>. Relative fluorescence was measured for each set of neurons by structure  
742 (i.e., LNV soma or s-LNV dorsal axonal projections) as integrated density of pixel  
743 intensity, and the average of both hemispheres was recorded for each brain. We  
744 quantified all images blind to treatment (species, genotype, and timepoint). We  
745 compared Pdf immunofluorescence between strains within photoperiod treatments  
746 using a Wilcoxon rank-sum test followed by post-hoc correction for multiple tests<sup>86</sup>.  
747 We did not compare between experiments as these flies were dissected, stained,  
748 and imaged separately. We repeated immunostainings throughout the morning  
749 peak to ensure replicability of the overall pattern of expression. These data cannot  
750 be pooled, however, as they are from a separate staining/imaging and produce  
751 different fluorescence measurements (arbitrary units).

752 To compare structural plasticity of s-LNV axonal projections between *D.*  
753 *melanogaster* and *D. sechellia*, we imaged the most dorsal projections during two  
754 timepoints in the light and dark phase (2 h and 14 h, respectively) at 40× with a 2×  
755 digital zoom. We performed a Scholl analysis, counting the number of axonal  
756 crossings with concentric 10 μm arcs using the Neuroanatomy Fiji plugin<sup>89</sup>. The  
757 number of axonal crossings was averaged per hemisphere for each brain and  
758 compared using a Wilcoxon rank-sum test. We performed this experiment in two  
759 replicates and pooled replicates for analysis as fluorescence intensity was not  
760 measured.

761

## 762 **Pdf gene region sequence comparisons**

763

764 We Sanger-sequenced the *Pdf* gene region using the oligonucleotides listed in  
765 Supplementary Table 3. The sequences were assembled and aligned in SnapGene  
766 software ([www.snapgene.com](http://www.snapgene.com)) using MUSCLE v3.8.1551<sup>90</sup> and then visually  
767 inspected for errors. When appropriate, sequences were translated to an amino  
768 acid alignment and visualized using Jalview<sup>91</sup>. For 5'-regulatory sequences, we  
769 used the R package phangorn to generate maximum likelihood trees<sup>92</sup>, using the  
770 modelTest function to identify the best fitting substitution model and performing  
771 standard bootstrapping to obtain support values. The MEME program was used to  
772 discover putative regulatory motifs common across all sequences<sup>47</sup>. We restricted  
773 this analysis to the top ten significant motifs identified.

774

775 **Population genetic analysis of the *Pdf* 5' regulatory sequences in *D.***  
776 ***melanogaster* and *D. sechellia***

777

778 To detect genomic patterns of clinal adaptation in the *Pdf* 5' sequences, we used  
779 a dataset of single nucleotide variants in globally distributed *D. melanogaster*  
780 populations<sup>48</sup>. We calculated the average MAF for each population in this region,  
781 and for the same-sized region upstream of the start codon of 6 control neuropeptide  
782 genes. Spearman's rho was used to correlate MAF with the latitude of the capital  
783 city in each country where the populations were sampled (precise latitudes were  
784 not available).

785

786 **Longevity assay**

787

788 To test for photoperiod-dependent differences in lifespan, we acclimated 1-day old  
789 *DmelCS*, *DmelOR*, *Dsec07* and *Dsec28* males to either 12:12 h LD or 16:8 h LD  
790 conditions. We held these flies in vials containing wheat flour-yeast-fruit juice media  
791 to which we added an additional mixture of instant *Drosophila* medium (Formula 4-  
792 24 blue, Carolina bio-supply) mixed with noni juice for *D. sechellia* and apple cider  
793 vinegar for *D. melanogaster*. Flies were transferred to fresh vials every 3 days to  
794 prevent the media from drying out. We recorded for each week-day the number of  
795 vials in which a fly died until all flies among one treatment per strain were dead. No  
796 significant differences were detected between strains within species (Fisher's exact  
797 test, all  $p > 0.05$ ), which were therefore pooled to represent the species for analysis.  
798 We compared cumulative survival probability using the R package 'survival'<sup>93</sup>.

799

800 **Copulation rate assays**

801

802 To test for photoperiod-dependent differences in copulation rate, we first  
803 acclimated 1-day old virgin *DmelCS*, *DmelOR*, *Dsec07* and *Dsec28* males and  
804 females to either 12:12 h LD or 16:8 h LD conditions for 4 days. For our short-term  
805 assay, we aspirated single females into 25 mm food vials containing wheat flour-  
806 yeast-fruit juice media, returned them to their respective photoperiods, and allowed  
807 them to recover for 24 h. The following day, 30 min after lights-on, we aspirated a  
808 single male of the same genotype into each tube, pushed the plug into the vial so  
809 that pairs had 2 cm above the food surface, forcing them to interact. We observed  
810 for copulation for 2 h, recording successfully and unsuccessfully copulating pairs.  
811 For our long-term assay, we similarly acclimated flies for 4 days, but aspirated  
812 male-female pairs of the same genotype into vials and returned them to their  
813 respective photoperiods. We transferred these pairs to new vials every 24 h, and  
814 scored copulation success per day based on the presence of offspring. Flies that  
815 produced no offspring over 7 days were considered to have never mated. We  
816 observed no differences between strains within species in either experiment  
817 (Fisher's exact test, all  $p = 1$ ), so these data were pooled to represent the species  
818 for analysis. Copulation frequencies within species between treatments were  
819 compared using a Wilcoxon rank-sum test.

820

821

822

823 **References**

824

- 825 1 Rieger, D., Stanewsky, R. & Helfrich-Forster, C. Cryptochrome, compound  
826 eyes, Hofbauer-Buchner eyelets, and ocelli play different roles in the  
827 entrainment and masking pathway of the locomotor activity rhythm in the  
828 fruit fly *Drosophila melanogaster*. *Journal of biological rhythms* **18**, 377-  
829 391, doi:10.1177/0748730403256997 (2003).
- 830 2 Auer, T. O., Shahandeh, M. P. & Benton, R. *Drosophila sechellia*: A  
831 Genetic Model for Behavioral Evolution and Neuroecology. *Annu Rev*  
832 *Genet* **55**, 527-554, doi:10.1146/annurev-genet-071719-020719 (2021).
- 833 3 Jones, C. D. The genetics of adaptation in *Drosophila sechellia*. *Genetica*  
834 **123**, 137-145 (2005).
- 835 4 Menegazzi, P. *et al.* Adaptation of Circadian Neuronal Network to  
836 Photoperiod in High-Latitude European *Drosophilids*. *Curr Biol* **27**, 833-  
837 839, doi:10.1016/j.cub.2017.01.036 (2017).
- 838 5 Bahn, J. H., Lee, G. & Park, J. H. Comparative analysis of Pdf-mediated  
839 circadian behaviors between *Drosophila melanogaster* and *D. virilis*.  
840 *Genetics* **181**, 965-975, doi:10.1534/genetics.108.099069 (2009).
- 841 6 Roca, I. T. *et al.* Shifting song frequencies in response to anthropogenic  
842 noise: a meta-analysis on birds and anurans. *Behavioral Ecology* **27**,  
843 1269-1274, doi:10.1093/beheco/arw060 (2016).
- 844 7 Andrew, N. R., Hart, R. A., Jung, M. P., Hemmings, Z. & Terblanche, J. S.  
845 Can temperate insects take the heat? A case study of the physiological  
846 and behavioural responses in a common ant, *Iridomyrmex purpureus*  
847 (Formicidae), with potential climate change. *J Insect Physiol* **59**, 870-880,  
848 doi:10.1016/j.jinsphys.2013.06.003 (2013).
- 849 8 Caldwell, A. J., While, G. M. & Wapstra, E. Plasticity of thermoregulatory  
850 behaviour in response to the thermal environment by widespread and  
851 alpine reptile species. *Animal Behaviour* **132**, 217-227,  
852 doi:10.1016/j.anbehav.2017.07.025 (2017).
- 853 9 Muraro, N. I., Pirez, N. & Ceriani, M. F. The circadian system: plasticity at  
854 many levels. *Neuroscience* **247**, 280-293,  
855 doi:10.1016/j.neuroscience.2013.05.036 (2013).
- 856 10 Emerson, K. J., Bradshaw, W. E. & Holzapfel, C. M. Concordance of the  
857 circadian clock with the environment is necessary to maximize fitness in  
858 natural populations. *Evolution* **62**, 979-983, doi:10.1111/j.1558-  
859 5646.2008.00324.x (2008).
- 860 11 Wang, G. *et al.* Clock genes and environmental cues coordinate  
861 *Anopheles* pheromone synthesis, swarming, and mating. *Science* **371**,  
862 411-415, doi:10.1126/science.abd4359 (2021).
- 863 12 Beaver, L. M. *et al.* Loss of circadian clock function decreases reproductive  
864 fitness in males of *Drosophila melanogaster*. *Proceedings of the National*  
865 *Academy of Sciences of the United States of America* **99**, 2134-2139,  
866 doi:10.1073/pnas.032426699 (2002).
- 867 13 Horn, M. *et al.* The Circadian Clock Improves Fitness in the Fruit Fly,  
868 *Drosophila melanogaster*. *Frontiers in physiology* **10**, 1374,  
869 doi:10.3389/fphys.2019.01374 (2019).
- 870 14 Hardeland, R. & Stange, G. Comparative studies on the circadian rhythms  
871 of locomotor activity of 40 *Drosophila* species. *Journal of Interdisciplinary*  
872 *Cycle Research* **4**, 353-359, doi:10.1080/09291017309359398 (1973).

- 873 15 Rieger, D., Peschel, N., Dusik, V., Glotz, S. & Helfrich-Forster, C. The  
874 ability to entrain to long photoperiods differs between 3 *Drosophila*  
875 *melanogaster* wild-type strains and is modified by twilight simulation.  
876 *Journal of biological rhythms* **27**, 37-47, doi:10.1177/0748730411420246  
877 (2012).
- 878 16 Beauchamp, M. *et al.* Closely Related Fruit Fly Species Living at Different  
879 Latitudes Diverge in Their Circadian Clock Anatomy and Rhythmic  
880 Behavior. *Journal of biological rhythms* **33**, 602-613,  
881 doi:10.1177/0748730418798096 (2018).
- 882 17 Bywalez, W. *et al.* The dual-oscillator system of *Drosophila melanogaster*  
883 under natural-like temperature cycles. *Chronobiol Int* **29**, 395-407,  
884 doi:10.3109/07420528.2012.668505 (2012).
- 885 18 Lachaise, D. *et al.* *Historical biogeography of the Drosophila melanogaster*  
886 *species subgroup*. 159-225 (Plenun Press, 1988).
- 887 19 Dean, M. D. & Ballard, J. W. Linking phylogenetics with population  
888 genetics to reconstruct the geographic origin of a species. *Mol Phylogenet*  
889 *Evol* **32**, 998-1009, doi:10.1016/j.ympev.2004.03.013 (2004).
- 890 20 Nitabach, M. N. & Taghert, P. H. Organization of the *Drosophila* circadian  
891 control circuit. *Curr Biol* **18**, R84-93, doi:10.1016/j.cub.2007.11.061 (2008).
- 892 21 Hardin, P. E. Molecular genetic analysis of circadian timekeeping in  
893 *Drosophila*. *Adv Genet* **74**, 141-173, doi:10.1016/B978-0-12-387690-  
894 4.00005-2 (2011).
- 895 22 Hermann-Luibl, C. & Helfrich-Forster, C. Clock network in *Drosophila*. *Curr*  
896 *Opin Insect Sci* **7**, 65-70, doi:10.1016/j.cois.2014.11.003 (2015).
- 897 23 Dubowy, C. & Sehgal, A. Circadian Rhythms and Sleep in *Drosophila*  
898 *melanogaster*. *Genetics* **205**, 1373-1397, doi:10.1534/genetics.115.185157  
899 (2017).
- 900 24 Stern, D. L. Identification of loci that cause phenotypic variation in diverse  
901 species with the reciprocal hemizyosity test. *Trends Genet* **30**, 547-554,  
902 doi:10.1016/j.tig.2014.09.006 (2014).
- 903 25 Vaze, K. M. & Helfrich-Forster, C. The Neuropeptide PDF Is Crucial for  
904 Delaying the Phase of *Drosophila's* Evening Neurons Under Long  
905 Zeitgeber Periods. *Journal of biological rhythms* **36**, 442-460,  
906 doi:10.1177/07487304211032336 (2021).
- 907 26 Yoshii, T. *et al.* The neuropeptide pigment-dispersing factor adjusts period  
908 and phase of *Drosophila's* clock. *J Neurosci* **29**, 2597-2610,  
909 doi:10.1523/JNEUROSCI.5439-08.2009 (2009).
- 910 27 Schlichting, M. *et al.* A Neural Network Underlying Circadian Entrainment  
911 and Photoperiodic Adjustment of Sleep and Activity in *Drosophila*. *J*  
912 *Neurosci* **36**, 9084-9096, doi:10.1523/JNEUROSCI.0992-16.2016 (2016).
- 913 28 Yoshii, T., Todo, T., Wulbeck, C., Stanewsky, R. & Helfrich-Forster, C.  
914 Cryptochrome is present in the compound eyes and a subset of  
915 *Drosophila's* clock neurons. *J Comp Neurol* **508**, 952-966,  
916 doi:10.1002/cne.21702 (2008).
- 917 29 Koh, K., Zheng, X. & Sehgal, A. JETLAG resets the *Drosophila* circadian  
918 clock by promoting light-induced degradation of TIMELESS. *Science* **312**,  
919 1809-1812, doi:10.1126/science.1124951 (2006).
- 920 30 Peschel, N., Chen, K. F., Szabo, G. & Stanewsky, R. Light-dependent  
921 interactions between the *Drosophila* circadian clock factors cryptochrome,

- 922 jetlag, and timeless. *Curr Biol* **19**, 241-247, doi:10.1016/j.cub.2008.12.042  
923 (2009).
- 924 31 Gunawardhana, K. L. & Hardin, P. E. VRILLE Controls PDF Neuropeptide  
925 Accumulation and Arborization Rhythms in Small Ventrolateral Neurons to  
926 Drive Rhythmic Behavior in *Drosophila*. *Curr Biol* **27**, 3442-3453,  
927 doi:10.1016/j.cub.2017.10.010 (2017).
- 928 32 Grima, B., Chelot, E., Xia, R. & Rouyer, F. Morning and evening peaks of  
929 activity rely on different clock neurons of the *Drosophila* brain. *Nature* **431**,  
930 869-873, doi:10.1038/nature02935 (2004).
- 931 33 Delventhal, R. *et al.* Dissection of central clock function in *Drosophila*  
932 through cell-specific CRISPR-mediated clock gene disruption. *Elife* **8**,  
933 e48308, doi:10.7554/eLife.48308 (2019).
- 934 34 Stoleru, D., Peng, Y., Agosto, J. & Rosbash, M. Coupled oscillators control  
935 morning and evening locomotor behaviour of *Drosophila*. *Nature* **431**, 862-  
936 868, doi:10.1038/nature02926 (2004).
- 937 35 Menegazzi, P. *et al.* A Functional Clock Within the Main Morning and  
938 Evening Neurons of *D. melanogaster* Is Not Sufficient for Wild-Type  
939 Locomotor Activity Under Changing Day Length. *Frontiers in physiology*  
940 **11**, 229, doi:10.3389/fphys.2020.00229 (2020).
- 941 36 Hermann, C. *et al.* The circadian clock network in the brain of different  
942 *Drosophila* species. *J Comp Neurol* **521**, 367-388, doi:10.1002/cne.23178  
943 (2013).
- 944 37 Park, J. H. *et al.* Differential regulation of circadian pacemaker output by  
945 separate clock genes in *Drosophila*. *Proceedings of the National Academy*  
946 *of Sciences of the United States of America* **97**, 3608-3613,  
947 doi:10.1073/pnas.97.7.3608 (2000).
- 948 38 Han, C., Jan, L. Y. & Jan, Y. N. Enhancer-driven membrane markers for  
949 analysis of nonautonomous mechanisms reveal neuron-glia interactions in  
950 *Drosophila*. *Proceedings of the National Academy of Sciences of the*  
951 *United States of America* **108**, 9673-9678, doi:10.1073/pnas.1106386108  
952 (2011).
- 953 39 Zhang, L. *et al.* DN1(p) circadian neurons coordinate acute light and PDF  
954 inputs to produce robust daily behavior in *Drosophila*. *Curr Biol* **20**, 591-  
955 599, doi:10.1016/j.cub.2010.02.056 (2010).
- 956 40 Liang, X., Holy, T. E. & Taghert, P. H. A Series of Suppressive Signals  
957 within the *Drosophila* Circadian Neural Circuit Generates Sequential Daily  
958 Outputs. *Neuron* **94**, 1173-1189 e1174, doi:10.1016/j.neuron.2017.05.007  
959 (2017).
- 960 41 Ryczek, N., Lys, A. & Makalowska, I. The Functional Meaning of 5'UTR in  
961 Protein-Coding Genes. *International journal of molecular sciences* **24**,  
962 doi:10.3390/ijms24032976 (2023).
- 963 42 Herrero, A. *et al.* Coupling Neuropeptide Levels to Structural Plasticity in  
964 *Drosophila* Clock Neurons. *Curr Biol* **30**, 3154-3166,  
965 doi:10.1016/j.cub.2020.06.009 (2020).
- 966 43 Ma, D. *et al.* A transcriptomic taxonomy of *Drosophila* circadian neurons  
967 around the clock. *Elife* **10**, doi:10.7554/eLife.63056 (2021).
- 968 44 Kula-Eversole, E. *et al.* Surprising gene expression patterns within and  
969 between PDF-containing circadian neurons in *Drosophila*. *Proceedings of*  
970 *the National Academy of Sciences of the United States of America* **107**,  
971 13497-13502, doi:10.1073/pnas.1002081107 (2010).

- 972 45 Long, X., Colonell, J., Wong, A. M., Singer, R. H. & Lionnet, T. Quantitative  
973 mRNA imaging throughout the entire *Drosophila* brain. *Nat Methods* **14**,  
974 703-706, doi:10.1038/nmeth.4309 (2017).
- 975 46 Fernandez, M. P., Berni, J. & Ceriani, M. F. Circadian remodeling of  
976 neuronal circuits involved in rhythmic behavior. *PLOS Biol.* **6**, e69,  
977 doi:10.1371/journal.pbio.0060069 (2008).
- 978 47 Bailey, T. L. & Elkan, C. Fitting a mixture model by expectation  
979 maximization to discover motifs in biopolymers. *Proc Int Conf Intell Syst*  
980 *Mol Biol* **2**, 28-36 (1994).
- 981 48 Bergland, A. O., Tobler, R., Gonzalez, J., Schmidt, P. & Petrov, D.  
982 Secondary contact and local adaptation contribute to genome-wide  
983 patterns of clinal variation in *Drosophila melanogaster*. *Mol. Ecol.* **25**,  
984 1157-1174, doi:10.1111/mec.13455 (2016).
- 985 49 Arguello, J. R., Laurent, S. & Clark, A. G. Demographic History of the  
986 Human Commensal *Drosophila melanogaster*. *Genome Biol. Evol.* **11**,  
987 844-854, doi:10.1093/gbe/evz022 (2019).
- 988 50 Khatib, L., Subasi, B. S., Fishman, B., Kapun, M. & Tauber, E. Unveiling  
989 Subtle Geographical Clines: Phenotypic Effects and Dynamics of Circadian  
990 Clock Gene Polymorphisms. *Biology* **12** (2023).
- 991 51 Lamaze, A. *et al.* A natural timeless polymorphism allowing circadian clock  
992 synchronization in "white nights". *Nat Commun* **13**, 1724,  
993 doi:10.1038/s41467-022-29293-6 (2022).
- 994 52 Tauber, E. *et al.* Natural selection favors a newly derived timeless allele in  
995 *Drosophila melanogaster*. *Science* **316**, 1895-1898,  
996 doi:10.1126/science.1138412 (2007).
- 997 53 Sawyer, L. A. *et al.* Natural variation in a *Drosophila* clock gene and  
998 temperature compensation. *Science* **278**, 2117-2120,  
999 doi:10.1126/science.278.5346.2117 (1997).
- 1000 54 Costanzo, K. S., Schelble, S., Jerz, K. & Keenan, M. The effect of  
1001 photoperiod on life history and blood-feeding activity in *Aedes albopictus*  
1002 and *Aedes aegypti* (Diptera: Culicidae). *J Vector Ecol* **40**, 164-171,  
1003 doi:10.1111/jvec.12146 (2015).
- 1004 55 Li, J. C. & Xu, F. Influences of light-dark shifting on the immune system,  
1005 tumor growth and life span of rats, mice and fruit flies as well as on the  
1006 counteraction of melatonin. *Biol Signals* **6**, 77-89, doi:10.1159/000109112  
1007 (1997).
- 1008 56 Amin, M. R., Suh, S. J. & Kwon, Y. J. Effects of photoperiod and  
1009 hibernation duration on the lifespan of *Bombus terrestris*. *Entomological*  
1010 *Research* **37**, 89-94, doi:10.1111/j.1748-5967.2007.00058.x (2007).
- 1011 57 Ducatez, S., Sol, D., Sayol, F. & Lefebvre, L. Behavioural plasticity is  
1012 associated with reduced extinction risk in birds. *Nature ecology & evolution*  
1013 **4**, 788-793, doi:10.1038/s41559-020-1168-8 (2020).
- 1014 58 Courtier-Orgogozo, V., Arnoult, L., Prigent, S. R., Wiltgen, S. & Martin, A.  
1015 Gephebase, a database of genotype-phenotype relationships for natural  
1016 and domesticated variation in Eukaryotes. *Nucleic Acids Res.* **48**, D696-  
1017 D703, doi:10.1093/nar/gkz796 (2020).
- 1018 59 Auer, T. O. *et al.* Olfactory receptor and circuit evolution promote host  
1019 specialization. *Nature* **579**, 402-408, doi:10.1038/s41586-020-2073-7  
1020 (2020).

- 1021 60 Leary, G. P. *et al.* Single mutation to a sex pheromone receptor provides  
1022 adaptive specificity between closely related moth species. *Proc. Natl.*  
1023 *Acad. Sci. USA* **109**, 14081-14086, doi:10.1073/pnas.1204661109 (2012).
- 1024 61 Wisotsky, Z., Medina, A., Freeman, E. & Dahanukar, A. Evolutionary  
1025 differences in food preference rely on Gr64e, a receptor for glycerol.  
1026 *Nature Neuroscience* **14**, 1534-1541, doi:10.1038/nn.2944 (2011).
- 1027 62 Baldwin, M. W. *et al.* Sensory biology. Evolution of sweet taste perception  
1028 in hummingbirds by transformation of the ancestral umami receptor.  
1029 *Science* **345**, 929-933, doi:10.1126/science.1255097 (2014).
- 1030 63 Seeholzer, L. F., Seppo, M., Stern, D. L. & Ruta, V. Evolution of a central  
1031 neural circuit underlies *Drosophila* mate preferences. *Nature* **559**, 564-569,  
1032 doi:10.1038/s41586-018-0322-9 (2018).
- 1033 64 Shafer, O. T. *et al.* Widespread receptivity to neuropeptide PDF throughout  
1034 the neuronal circadian clock network of *Drosophila* revealed by real-time  
1035 cyclic AMP imaging. *Neuron* **58**, 223-237,  
1036 doi:10.1016/j.neuron.2008.02.018 (2008).
- 1037 65 Carroll, S. B. Evo-devo and an expanding evolutionary synthesis: a genetic  
1038 theory of morphological evolution. *Cell* **134**, 25-36, doi:S0092-  
1039 8674(08)00817-9 [pii]10.1016/j.cell.2008.06.030 (2008).
- 1040 66 Ding, K. *et al.* Imaging neuropeptide release at synapses with a genetically  
1041 engineered reporter. *Elife* **8**, e46421, doi:10.7554/eLife.46421 (2019).
- 1042 67 Hidalgo, S., Anguiano, M., Tabuloc, C. A. & Chiu, J. C. Seasonal cues act  
1043 through the circadian clock and pigment-dispersing factor to control EYES  
1044 ABSENT and downstream physiological changes. *Curr Biol* **33**, 1006-1008,  
1045 doi:10.1016/j.cub.2023.02.028 (2023).
- 1046 68 Renn, S. C., Park, J. H., Rosbash, M., Hall, J. C. & Taghert, P. H. A pdf  
1047 neuropeptide gene mutation and ablation of PDF neurons each cause  
1048 severe abnormalities of behavioral circadian rhythms in *Drosophila*. *Cell*  
1049 **99**, 791-802, doi:10.1016/s0092-8674(00)81676-1 (1999).
- 1050 69 Duhart, J. M. *et al.* Circadian Structural Plasticity Drives Remodeling of E  
1051 Cell Output. *Curr Biol* **30**, 5040-5048, doi:10.1016/j.cub.2020.09.057  
1052 (2020).
- 1053 70 Prieto-Godino, L. L., Schmidt, H. R. & Benton, R. Molecular reconstruction  
1054 of recurrent evolutionary switching in olfactory receptor specificity. *Elife* **10**,  
1055 e69732, doi:10.7554/eLife.69732 (2021).
- 1056 71 Prieto-Godino, L. L. *et al.* Evolution of Acid-Sensing Olfactory Circuits in  
1057 *Drosophilids*. *Neuron* **93**, 661-676, doi:10.1016/j.neuron.2016.12.024  
1058 (2017).
- 1059 72 Alvarez-Ocana, R. *et al.* Odor-regulated oviposition behavior in an  
1060 ecological specialist. *Nat Commun* **14**, 3041, doi:10.1038/s41467-023-  
1061 38722-z (2023).
- 1062 73 Ibbá, I., Angioy, A. M., Hansson, B. S. & Dekker, T. Macroglomeruli for fruit  
1063 odors change blend preference in *Drosophila*. *Die Naturwissenschaften*  
1064 **97**, 1059-1066, doi:10.1007/s00114-010-0727-2 (2010).
- 1065 74 Dekker, T., Ibbá, I., Siju, K. P., Stensmyr, M. C. & Hansson, B. S. Olfactory  
1066 shifts parallel superspecialism for toxic fruit in *Drosophila melanogaster*  
1067 sibling, *D. sechellia*. *Curr Biol* **16**, 101-109 (2006).
- 1068 75 Reisenman, C. E., Wong, J., Vedagarbha, N., Lavelo, C. & Scott, K. Taste  
1069 adaptations associated with host specialization in the specialist *Drosophila*  
1070 *sechellia*. *J Exp Biol* **226**, jeb244641, doi:10.1242/jeb.244641 (2023).

- 1071 76 Karpati, Z., Deutsch, F., Kiss, B. & Schmitt, T. Seasonal changes in  
1072 photoperiod and temperature lead to changes in cuticular hydrocarbon  
1073 profiles and affect mating success in *Drosophila suzukii*. *Sci Rep* **13**, 5649,  
1074 doi:10.1038/s41598-023-32652-y (2023).
- 1075 77 Razafimandimbison, S. G., McDowell, T. D., Halford, D. A. & Bremer, B.  
1076 Origin of the pantropical and nutraceutical *Morinda citrifolia* L. (Rubiaceae):  
1077 comments on its distribution range and circumscription *Journal of*  
1078 *Biogeography* **37**, 520-529 (2010).
- 1079 78 Nair, S., Bahn, J. H., Lee, G., Yoo, S. & Park, J. H. A Homeobox  
1080 Transcription Factor Scarecrow (SCRO) Negatively Regulates Pdf  
1081 Neuropeptide Expression through Binding an Identified cis-Acting Element  
1082 in *Drosophila melanogaster*. *Mol Neurobiol* **57**, 2115-2130,  
1083 doi:10.1007/s12035-020-01874-w (2020).
- 1084 79 Cook, R. K. *et al.* The generation of chromosomal deletions to provide  
1085 extensive coverage and subdivision of the *Drosophila melanogaster*  
1086 genome. *Genome Biol* **13**, R21, doi:10.1186/gb-2012-13-3-r21 (2012).
- 1087 80 Shahandeh, M. P. & Turner, T. L. The complex genetic architecture of  
1088 male mate choice evolution between *Drosophila* species. *Heredity (Edinb)*  
1089 **124**, 737-750, doi:10.1038/s41437-020-0309-9 (2020).
- 1090 81 Zhou, J., Yu, W. & Hardin, P. E. CLOCKWORK ORANGE Enhances  
1091 PERIOD Mediated Rhythms in Transcriptional Repression by Antagonizing  
1092 E-box Binding by CLOCK-CYCLE. *PLOS Genet.* **12**, e1006430,  
1093 doi:10.1371/journal.pgen.1006430 (2016).
- 1094 82 Chiu, J. C., Low, K. H., Pike, D. H., Yildirim, E. & Edery, I. Assaying  
1095 locomotor activity to study circadian rhythms and sleep parameters in  
1096 *Drosophila*. *J Vis Exp*, e2157, doi:10.3791/2157 (2010).
- 1097 83 Geissmann, Q., Garcia Rodriguez, L., Beckwith, E. J. & Gilestro, G. F.  
1098 Rethomics: An R framework to analyse high-throughput behavioural data.  
1099 *PLOS ONE* **14**, e0209331, doi:10.1371/journal.pone.0209331 (2019).
- 1100 84 Yuan, Y., Padilla, M. A., Clark, D. & Yadlapalli, S. Streamlined single-  
1101 molecule RNA-FISH of core clock mRNAs in clock neurons in whole mount  
1102 *Drosophila* brains. *Frontiers in physiology* **13**, 1051544,  
1103 doi:10.3389/fphys.2022.1051544 (2022).
- 1104 85 Bahry, E. *et al.* RS-FISH: precise, interactive, fast, and scalable FISH spot  
1105 detection. *Nat Methods* **19**, 1563-1567, doi:10.1038/s41592-022-01669-y  
1106 (2022).
- 1107 86 Holm, S. A Simple Sequentially Rejective Multiple Test Procedure.  
1108 *Scandinavian Journal of Statistics* **6**, 65-70 (1979).
- 1109 87 Ostrovsky, A., Cachero, S. & Jefferis, G. Clonal analysis of olfaction in  
1110 *Drosophila*: immunochemistry and imaging of fly brains. *Cold Spring Harb*  
1111 *Protoc* **2013**, 342-346, doi:10.1101/pdb.prot071720 (2013).
- 1112 88 Schindelin, J. *et al.* Fiji: an open-source platform for biological-image  
1113 analysis. *Nat Methods* **9**, 676-682, doi:10.1038/nmeth.2019 (2012).
- 1114 89 Ferreira, T. A. *et al.* Neuronal morphometry directly from bitmap images.  
1115 *Nat Methods* **11**, 982-984, doi:10.1038/nmeth.3125 (2014).
- 1116 90 Edgar, R. C. MUSCLE: multiple sequence alignment with high accuracy  
1117 and high throughput. *Nucleic Acids Res.* **32**, 1792-1797,  
1118 doi:10.1093/nar/gkh34032/5/1792 [pii] (2004).

- 1119 91 Procter, J. B. *et al.* Alignment of Biological Sequences with Jalview.  
1120 *Methods Mol Biol* **2231**, 203-224, doi:10.1007/978-1-0716-1036-7\_13  
1121 (2021).
- 1122 92 Schliep, K. P. phangorn: phylogenetic analysis in R. *Bioinformatics* **27**,  
1123 592-593, doi:10.1093/bioinformatics/btq706 (2011).
- 1124 93 Therneau, T. M. & Grambsch, P. M. *Modeling survival data : extending the*  
1125 *Cox model*. (Springer, 2000).
- 1126 94 Matute, D. R., Gavin-Smyth, J. & Liu, G. Variable post-zygotic isolation in  
1127 *Drosophila melanogaster/D. simulans* hybrids. *J Evol Biol* **27**, 1691-1705,  
1128 doi:10.1111/jeb.12422 (2014).  
1129  
1130

1131 **Figure legends**

1132

1133 **Fig. 1. *D. sechellia* displays reduced circadian plasticity and lower morning**  
1134 **activity than *D. melanogaster*.**

- 1135 a, Left: phylogeny of the *Drosophila melanogaster* sub-group. Right: modern  
1136 ranges of the focal species of this study, *D. melanogaster* (*Dmel*) and *D.*  
1137 *sechellia* (*Dsec*), are indicated by the shaded regions (blue and orange,  
1138 respectively) on the map, with the approximate collection sites of the wild-  
1139 type strains used.
- 1140 b, Approximate seasonal photoperiod variation at the collection sites of the *D.*  
1141 *melanogaster* (left) and *D. sechellia* strains (right).
- 1142 c, Top: mean normalized activity of two *D. melanogaster* (CS and OR, blue) and  
1143 two *D. sechellia* (07 and 28, orange) strains under the indicated  
1144 photoperiods. Plots depict normalized average activity of the last 4 days of  
1145 a 7-day photoperiod, for extended photoperiods, following 7 days of 12:12 h  
1146 LD. Vertical dashed lines indicate the average timing of the evening peak  
1147 for each strain. Here and elsewhere, yellow and grey bars indicate timing of  
1148 lights-on and lights-off, respectively. Overall, *D. sechellia* strains were  
1149 slightly less active than *D. melanogaster* strains. Bottom: box plots depict  
1150 evening peak time quantifications for individual flies under each  
1151 photoperiod. Here and elsewhere, box plots show the median (bold line),  
1152 interquartile range (box), and whiskers represent the final quartiles. All data  
1153 points are shown overlaid on box plots. Outliers are points that fall beyond  
1154 the box plot whiskers. Letters indicate significant differences:  $p < 0.05$   
1155 (pairwise Wilcoxon test with Bonferroni correction). Sample sizes (numbers  
1156 of individual flies) are as follows: 12:12 h LD: CS (18), OR (21), 07 (24), 28  
1157 (19); 14:10 h LD: CS (22), OR (22), 07 (19), 28 (13); 16:8 h LD: CS (18), OR  
1158 (21), 07 (24), 28 (19); 18:10 h LD: CS (22), OR (23), 07 (21), 28 (11); 20:4  
1159 h LD: CS (21), OR (22), 07 (19), 28 (18).
- 1160 d, Mean normalized activity of *D. melanogaster* and *D. sechellia* strains under  
1161 a 12:12 h LD cycle during the morning activity peak (same data from c.  
1162 restricted to -6 to 6 h). Left: plots depict average activity of the last 4 days of  
1163 a 7-day recording period. Dashed boxes highlight the pre-dawn period, 3 h  
1164 before lights-on. Right: mean normalized activity of individual flies within this  
1165 pre-dawn period. Letters indicate significant differences:  $p < 0.001$  (pairwise  
1166 Wilcoxon test with Bonferroni correction). Sample sizes as follows: CS (89),  
1167 OR (93), 07 (95), 28 (91).
- 1168 e, Double plotted actograms depicting the transition from the last 2 days of  
1169 12:12 h LD to the first 2 days of constant darkness (DD) for each strain.  
1170 Dashed boxes highlight morning activity peak period during DD, 3 h before  
1171 and after subjective lights-on. Sample sizes as follows: CS (29), OR (32), 07  
1172 (29), 28 (22). Grey bars indicate timing of subjective lights-on during DD.
- 1173 f, Morning peak time, in hours from lights-on, for individual flies from d. Letters  
1174 indicate significant differences:  $p < 0.001$  (pairwise Wilcoxon test with  
1175 Bonferroni correction).

1176

1177

1178

1179 **Fig. 2. A screen of circadian clock genes reveals distinct genetic**  
1180 **architectures underlying interspecific differences in plasticity and morning**  
1181 **activity.**

- 1182 a, Molecular components of the circadian clock in *D. melanogaster*.  
1183 b, Crossing schemes used to generate hemizygous test hybrids, heterozygous  
1184 control hybrids, and hemizygous *D. melanogaster* flies in a controlled  
1185 genetic background. The fourth (“dot”) chromosome is not shown.  
1186 c, Schematics illustrating the sought-after behavioural phenotypes of test  
1187 hybrids, and anticipated phenotypes of control hybrids and hemizygous *D.*  
1188 *melanogaster* controls: positive candidate gene test hybrids, but not  
1189 corresponding controls, will display reduced circadian plasticity and/or  
1190 reduced morning activity.  
1191 d, Mean normalized activity of the indicated control and hybrid genotypes under  
1192 a 16:8 h LD cycle. Plots depict average activity of the last 4 days of a 7-day  
1193 extended photoperiod, following 7 days of 12:12 h LD. Vertical dashed lines  
1194 indicate the average timing of the evening peak for each strain. Sample  
1195 sizes as follows: CS<sup>W</sup> (16), Pdf<sup>01</sup>/CS<sup>W</sup> (47), 07/CS<sup>W</sup> (25), 28/CS<sup>W</sup> (23),  
1196 07/Pdf<sup>01</sup> (37), 28/Pdf<sup>01</sup>(40), 07 (24), 28 (19). Full screen results are shown  
1197 in Extended Data Fig. 3.  
1198 e, Evening peak time for the flies depicted in d. Asterisks indicate significant  
1199 differences: \* = p < 0.05 and \*\*\* = p < 0.001 (Wilcoxon tests with Bonferroni  
1200 correction). Comparisons were made only between control and test hybrids  
1201 of the same genetic backgrounds.  
1202 f, Mean normalized activity of the indicated genotypes under a 12:12 h LD cycle,  
1203 illustrating the screened mutations displaying reduced morning anticipation  
1204 in test hybrids. Dashed boxes highlight the pre-dawn area used to quantify  
1205 morning anticipation. Full screen results are shown in Extended Data Fig. 4.  
1206 g, Mean normalized pre-dawn activity for the genotypes in f. Asterisks indicate  
1207 significant differences: \*\* = p < 0.01 and \*\*\* = p < 0.001 (Wilcoxon tests  
1208 comparing each test hybrid to the control hybrid strain (07/w<sup>1118</sup>) with  
1209 Bonferroni correction). Top right: the circadian molecular network in which  
1210 screen hits for morning anticipating are highlighted in green; genes in light  
1211 grey were unable to be tested (see Methods).

1212  
1213 **Fig. 3. Species-specific cis-regulatory elements impact Pdf expression and**  
1214 **have the potential to impact behaviour.**

- 1215 a, Schematic of the circadian clock network in *D. melanogaster*, which is  
1216 composed of ~75 neurons in each brain hemisphere that are divided into  
1217 distinct groups. The groups comprising the morning and evening cells are  
1218 indicated on the left and right hemispheres, respectively. Pdf-positive small  
1219 and large ventrolateral neurons (s-LNvs and l-LNvs) are highlighted in  
1220 purple.  
1221 b, Immunofluorescence for Pdf (green) and Cadherin-N (magenta) on whole-  
1222 mount brains of the indicated strains at 2 h under 12:12 h LD conditions.  
1223 c, Representative images of reporter expression visualized by Pdf (left) and  
1224 GFP immunofluorescence (middle) showing faithful labelling (merge, right)  
1225 of s-LNvs and l-LNvs for both the *D. melanogaster* (top) and *D. sechellia*  
1226 (bottom) Pdf 5'-regulatory regions. For b and c, scale bars, 100 μm.  
1227 d, Top: Schematic illustrating the average activity patterns of *D. melanogaster*  
1228 and *D. sechellia* during behaviourally relevant time points (labelled with

- 1229 arrowheads) within the evening peaks under 12:12 h LD conditions where  
1230 we analyzed *Pdf* expression. These summaries were derived from the data  
1231 in Fig. 1c-d. Bottom-left: representative images of GFP immunofluorescence  
1232 in the l-LNVs for the *D. melanogaster* and *D. sechellia Pdf* 5'-regulatory  
1233 sequence-GFP reporter strains under 12:12 h LD at one time point (10 h).  
1234 Bottom-right: GFP fluorescence quantifications at 5 time points spanning the  
1235 evening activity peak period.
- 1236 **e**, Top: Schematic illustrating the average activity patterns of *D. melanogaster*  
1237 and *D. sechellia* during behaviourally relevant time points (labelled with  
1238 arrowheads) within the evening peaks under 16:8 h LD conditions where we  
1239 analyzed *Pdf* expression. Bottom-left: representative images of GFP  
1240 reporter immunofluorescence in the l-LNVs for the *D. melanogaster* and *D.*  
1241 *sechellia* strains under 16:8 h LD at one time point (10 h). Bottom-right: GFP  
1242 fluorescence quantifications at 5 time points spanning the evening activity  
1243 peak period.
- 1244 **f**, Top: Schematic illustrating the average activity patterns of *D. melanogaster*  
1245 and *D. sechellia* during behaviourally relevant time points (labelled with  
1246 arrowheads) within the morning peaks under 12:12 h LD conditions where  
1247 we analyzed *Pdf* expression. Bottom-left: representative images of GFP  
1248 immunofluorescence in the s-LNV axon terminals for the *D. melanogaster*  
1249 and *D. sechellia Pdf* reporter strains at one time point (-2 h). We observed  
1250 the same general pattern when measuring fluorescence in the s-LNV soma.  
1251 Bottom-right: GFP fluorescence quantifications at 4 time points spanning the  
1252 morning activity peak period. For **d-f**, N = 5 for each strain and time point.  
1253 Despite weak signal in some *D. sechellia* images, the projections were easily  
1254 identified in thresholded images.
- 1255 **g**, Mean normalized activity of the indicated *D. melanogaster* genotypes under  
1256 a 16:8 h LD cycle. Plots depict average activity of the last 4 days of a 7-day  
1257 extended photoperiod, following 7 days of 12:12 h LD. Vertical dashed lines  
1258 indicate the average timing of the evening peak for each strain. Sample  
1259 sizes as follows: *DmelPdf-Gal4/+* (28), *DsecPdf-Gal4/+* (28), *UAS-Pdf<sup>RNAi</sup>/+*  
1260 *(16)*, *DmelPdf-Gal4/UAS-Pdf<sup>RNAi</sup>* (31), *DsecPdf-Gal4/UAS-Pdf<sup>RNAi</sup>* (24).
- 1261 **h**, Evening peak time for the flies shown in **g**.
- 1262 **i**, Mean normalized activity of the indicated *D. melanogaster* genotypes under  
1263 a 12:12 h LD cycle. Plots depict average activity of the last 4 days of a 7-  
1264 day recording period. Dashed boxes highlight the pre-dawn period, 3 h  
1265 before lights-on. Sample sizes as follows: *DmelPdf-Gal4/+* (31), *DsecPdf-*  
1266 *Gal4/+* (29), *UAS-Pdf<sup>RNAi</sup>/+* (47), *DmelPdf-Gal4/UAS-Pdf<sup>RNAi</sup>* (34), *DsecPdf-*  
1267 *Gal4/UAS-Pdf<sup>RNAi</sup>* (30).
- 1268 **j**, Mean normalized pre-dawn activity for the genotypes in **i**.
- 1269 For **d-f**, Lines connect medians of each time point within genotypes. Scale bars,  
1270 10  $\mu$ m.
- 1271 For **d-f**, **h** and **j**, Asterisks indicate significant differences: \* =  $p < 0.05$  and \*\*\* =  
1272  $p < 0.001$  (Wilcoxon tests with Bonferroni correction).
- 1273

1274 **Fig. 4. Pdf expression differences observed between *D. melanogaster* and *D.***  
1275 ***sechellia*.**

- 1276 **a**, Left: representative images of *Pdf* smFISH in the l-LNV soma in the CS and  
1277 07 strains under 12:12 h LD at one time point (14 h), with RNA spots (green)

1278 identified by RS-FISH. Right: quantifications of RNA spots at 5 time points  
1279 spanning the evening activity peak period.  
1280 **b**, Left: representative images of *Pdf* smFISH in the l-LNv soma in the CS and  
1281 07 strains under 16:8 h LD at one time point (14 h), with RNA spots (green)  
1282 identified by RS-FISH. Left: quantifications of RNA spots in the CS and 07  
1283 strains under 16:8 h LD at 5 time points spanning the evening activity peak  
1284 period.  
1285 **c**, Left: representative images of smFISH in the s-LNv soma for the CS and 07  
1286 strains under 12:12 h LD at one time point (-2 h) with RNA spots identified  
1287 by RS-FISH. Right: quantifications of RNA spots in the 07 and CS strains at  
1288 4 time points spanning the pre-dawn period.  
1289 **d**, Left: representative images of Pdf immunofluorescence in the s-LNv axon  
1290 terminals for the CS and 07 strains at one time point (-4 h). Right:  
1291 quantifications of Pdf signals at 4 time points spanning the morning activity  
1292 peak period.  
1293 **e**, Left: representative images of Pdf immunofluorescence in the s-LNv cell  
1294 bodies for the CS and 07 strains at one time point (2 h). Right: quantifications  
1295 of Pdf signals at 4 time points spanning the morning activity peak period.  
1296 **f**, Left: representative images of Pdf immunofluorescence in the s-LNv axon  
1297 terminals for the CS and 07 strains during the day (2 h) and night (14 h).  
1298 Right: quantifications of axonal branching complexity quantifications.  
1299 For **a-f**, N = 5 brains per strain per time point. Plotted values are the average of  
1300 left and right hemispheres. Lines connect medians of each time point within  
1301 genotypes. Asterisks indicate significant differences: \* =  $p < 0.05$  and \*\*\* =  
1302  $p < 0.001$  (Wilcoxon tests with Bonferroni correction). All scale bars, 10  $\mu\text{m}$ .  
1303

1304 **Fig. 5. Evidence for selection on the *Pdf* 5'-regulatory sequence and fitness**  
1305 **effects of circadian plasticity loss.**

1306 **a**, A midpoint rooted maximum likelihood phylogeny of *Pdf* 5'-regulatory  
1307 sequences from 10 *D. melanogaster* (blue), 6 *D. sechellia* (orange), and 5  
1308 *D. simulans* (grey) strains. Bootstrap support values are shown for key  
1309 internal nodes (100 bootstraps). The species tree is depicted at the bottom  
1310 left for comparison.  
1311 **b**, A motif analysis of the *Pdf* 5'-regulatory sequences from **a**. The *Pdf* start  
1312 codon is on the right, and the different types of predicted regulatory motifs  
1313 for each species are shown as distinct colored boxes on the + or - strand.  
1314 Species-specific diagrams depict all motifs found for each species. Motifs  
1315 observed in *D. melanogaster* and *D. simulans* but absent in all *D. sechellia*  
1316 sequences are marked with downward facing arrows; one motif unique to all  
1317 sequences of *D. sechellia* is marked with an upward facing arrow. No  
1318 variation in motif location was observed among the 6 *D. sechellia* strains.  
1319 **c**, Left: the 13 *D. melanogaster* populations selected from Ref.<sup>48</sup> and the  
1320 approximate latitude of their collection sites. Right: plot of minor allele  
1321 frequency in the *Pdf* 5'-regulatory sequences (blue) of these 13 populations  
1322 against latitude, revealing a significant positive correlation (Spearman's rho  
1323 = 0.77). No such correlation is observed for the putative 5'-regulatory  
1324 sequences of 6 control neuropeptide genes (grey); detailed data points are  
1325 shown in Extended Data Fig. 8.  
1326 **d**, Average minor allele frequency of variable sites from the analysis in **c** in the  
1327 laboratory *D. sechellia* and *D. melanogaster* lines from **a**. Variable sites are

- 1328 significantly underrepresented in *D. sechellia* relative to *D. melanogaster*  
1329 strains ( $p < 0.05$ , Fisher's exact test).
- 1330 **e**, Cumulative survival probability for *D. melanogaster* (*Dme*CS + *Dme*OR,  
1331 blue) and *D. sechellia* (*Dsec*07 + *Dsec* 28, orange) maintained at 12:12 h  
1332 LD (circles) or 16:8 h LD (squares) for 52 days. No significant differences  
1333 were observed between strains of the same species by photoperiod, and  
1334 were thus pooled (Fisher's exact test, all  $p > 0.05$ ). Pooled data were  
1335 compared between photoperiods within species using a log-rank test.
- 1336 **f**, Percent of copulating pairs observed for *D. melanogaster* (*Dme*CS +  
1337 *Dme*OR, blue) and *D. sechellia* (07 + 28, orange) after 2 h for flies  
1338 acclimated to 12:12 h LD (left) compared to 16:8 h LD (right, Wilcoxon test).  
1339 No significant differences were observed between strains of the same  
1340 species by photoperiod, and were thus pooled (Fisher's exact test, all  $p =$   
1341 1). Sample sizes as follows: *D. melanogaster* 12:12 h LD (22), *D.*  
1342 *melanogaster* 16:8 h LD (26), *D. sechellia* 12:12 h LD (29), and *D. sechellia*  
1343 16:8 h LD (32).
- 1344 **g**, Same as **f**, except after 3 days (left) or 7 days (right). Sample sizes as follows:  
1345 *D. melanogaster* 12:12 h LD (26), *D. melanogaster* 16:8 h LD (31), *D.*  
1346 *sechellia* 12:12 h LD (36), and *D. sechellia* 16:8 h LD (38).
- 1347 **h**, Schematic of the main findings of this work: the equatorial species *D.*  
1348 *sechellia* has lost circadian plasticity, in part through *cis*-regulatory changes  
1349 in the *Pdf* 5' region, which lead to less dynamic expression.
- 1350 For **c**, **e-g**, Asterisks indicate significant differences: \* =  $p < 0.05$ , \*\* =  $p < 0.01$ ,  
1351 and \*\*\* =  $p < 0.001$ .

1352

1353 **Extended Data Fig. 1. *D. melanogaster* and *D. sechellia* strains exhibit ~24**  
1354 **h periods.** Periodogram analysis from 5 days of constant darkness (DD) for *D.*  
1355 *melanogaster* (CS and OR) and *D. sechellia* (07 and 28) strains. Period  
1356 estimates: CS (24.36 h), OR (23.45 h), 07 (23.16 h), 28 (23.57 h). Sample sizes  
1357 as in Fig. 1e

1358

1359 **Extended Data Fig. 2. Tropical *D. melanogaster*, *D. simulans* and *D.***  
1360 ***mauritiana* strains display prominent circadian plasticity and morning**  
1361 **anticipation.**

- 1362 **a**, Top: mean normalized activity of two recently-collected strains of *D.*  
1363 *melanogaster* (LZV L72 and LZV L76, from the Lower Zambezi Valley), *D.*  
1364 *simulans* (MD221 and MD242, from Madagascar) and *D. mauritiana*  
1365 (*Dmau*90 and *Dmau*91, from Mauritius) under the indicated photoperiods.  
1366 Plots depict average activity of the last 4 days of a 7-day recording period.  
1367 Dashed lines highlight the average evening peak time. Bottom: evening  
1368 peak time for these flies. The orange line depicts the median evening peak  
1369 time of individuals of both *D. sechellia* strains (from Fig. 1c). Sample sizes  
1370 as follows: LZV L72 (29), LZV L74 (46), MD221 (27), MD242(34), *Dmau*90  
1371 (19), *Dmau*91 (28).
- 1372 **b**, Top: mean normalized activity of the same strains as in **a** under a 12:12 h LD  
1373 cycle (same as in **a**). Plots depict average activity of the last 4 days of a 7-  
1374 day recording period. Dashed boxes highlight the pre-dawn period, 3 h  
1375 before lights-on. Bottom: Mean normalized activity of individual flies within  
1376 this pre-dawn period. Sample sizes as follows: LZV L72 (41), LZV L74 (61),  
1377 MD221 (57), MD242 (52), *Dmau*90 (33), *Dmau*91 (34). The orange line

1378 depicts the median pre-dawn activity of individuals of both *D. sechellia*  
1379 strains (from Fig. 1d).

1380

1381 **Extended Data Fig. 3. Screen results for the genetic basis of interspecific**  
1382 **differences in circadian plasticity.**

1383 **a,** Mean normalized activity of the indicated control and hybrid genotypes under  
1384 a 16:8 h LD cycle. Plots depict average activity of the last 4 days of a 7-day  
1385 extended photoperiod, following 7 days of 12:12 h LD. Vertical dashed lines  
1386 indicate the average timing of the evening peak for each strain. Sample  
1387 sizes as follows: *w<sup>1118</sup>* (22), *07/w<sup>1118</sup>* (53), *07/CCHa1* (34), *07/Clk* (20),  
1388 *07/cwo* (16), *07/cyc* (33), *07/Cry* (21), *07/Fer2* (17), *07/Hr38* (50), *07/IITP*  
1389 (*23*), *07/Jet* (22), *07/Pdf* (37), *07/PDP1* (4), *07/Rh7* (16), *07/scro* (22), *07/vri*  
1390 (23).

1391 **b,** Evening peak time for the flies depicted in **a**. Asterisks indicate significant  
1392 differences: \*\*  $p < 0.01$  and \*\*\* =  $p < 0.001$  (Wilcoxon tests comparing each  
1393 test hybrid to the control hybrid strain (*07/w<sup>1118</sup>*) with Bonferroni correction).  
1394 n.s. = not significantly different. The orange line marks the median evening  
1395 peak delay of the *D. sechellia* parental strain (07).

1396 **c,** Mean normalized activity of the indicated control and hybrid genotypes under  
1397 a 16:8 h LD cycle. Plots depict average activity of the last 4 days of a 7-day  
1398 extended photoperiod, following 7 days of 12:12 h LD. Vertical dashed lines  
1399 indicate the average timing of the evening peak for each strain. Sample  
1400 sizes as follows: *w<sup>1118</sup>* (22), *28/w<sup>1118</sup>* (31), *28/CCHa1* (4), *28/Clk* (17), *28/cwo*  
1401 (*27*), *28/cyc* (52), *28/Cry* (28), *28/Fer* (8), *28/Hr38* (23), *28/ltp* (25), *28/Jet*  
1402 (*16*), *28/Pdf* (40), *28/scro* (31), *28/vri* (29), *28* (19).

1403 **d,** Evening peak time for the flies depicted in **c**. Asterisks indicate significant  
1404 differences: \* =  $p < 0.05$  (Wilcoxon tests comparing each test hybrid to the  
1405 control hybrid strain (*28/w<sup>1118</sup>*) with Bonferroni correction). Red asterisks  
1406 denote a significant increase in circadian plasticity. n.s. = not significantly  
1407 different. The orange line marks the median evening peak delay of the *D.*  
1408 *sechellia* parental strain (28).

1409 **e,** Mean normalized activity of the indicated hemizygous *D. melanogaster*  
1410 genotypes that displayed an effect in both hybrid backgrounds under a 16:8  
1411 h LD cycle. Plots depict average activity of the last 4 days of a 7-day  
1412 extended photoperiod, following 7 days of 12:12 h LD. Vertical dashed lines  
1413 indicate the average timing of the evening peak for each strain. Sample  
1414 sizes as follows: *w<sup>1118</sup>* (22), *Clk/w<sup>1118</sup>* (6), *Pdf/w<sup>1118</sup>* (37).

1415 **f,** Evening peak time for the flies depicted in **e**. Asterisks indicate significant  
1416 differences: \*\*\* =  $p < 0.001$  and \*\* =  $p < 0.01$  (Wilcoxon tests comparing  
1417 each test hemizygote to the control strain (*w<sup>1118</sup>*) with Bonferroni correction).  
1418 Red asterisks denote a significant increase in circadian plasticity.

1419 **g,** Summary of the overlapping hits. *A priori*, we considered the strongest  
1420 candidates would display a reduction in circadian plasticity in both *Dsec07*  
1421 and *Dsec28* hybrids, but not in *w<sup>1118</sup>* hemizygotes; only *Pdf* fulfilled these  
1422 criteria. Note: the *Clk* mutant used in this screen is a dominant negative  
1423 allele, and thus we expect the behaviour of *Clk/w<sup>1118</sup>* mutants to display a  
1424 total *Clk* loss-of-function phenotype. Interestingly, we do not observe this  
1425 phenotype in either test hybrid genotype, indicating divergence of the *Clk*  
1426 locus between species. If and how this divergence affects behaviour  
1427 requires subsequent investigation.

1428

1429

**Extended Data Fig. 4. Screen results for the genetic basis of interspecific differences in morning anticipation.**

1430

1431

a, Mean normalized activity of the indicated genotypes under a 12:12 h LD cycle. Dashed boxes highlight the pre-dawn area used to quantify morning anticipation. Sample sizes as follows:  $w^{1118}$  (78), 07/ $w^{1118}$  (69), 07/*CCHa1* (21), 07/*Clk* (19), 07/*cwo* (43), 07/*cyc* (43), 07/*Cry* (26), 07/*Fer* (18), 07/*Hr38* (87), 07/*IITP* (23), 07/*Jet* (49), 07/*Pdf* (42), 07/*PDP1* (23), 07/*Rh7* (33), 07/*scro* (58), 07/*vri* (28), 07 (40).

1432

1433

1434

1435

1436

1437

b, Mean normalized pre-dawn activity for the genotypes in A. Asterisks indicate significant differences: \*\* =  $p < 0.01$  and \*\*\* =  $p < 0.001$  (Wilcoxon tests comparing each test hybrid to the control hybrid strain (07/ $w^{1118}$ ) with Bonferroni correction). Red asterisks denote a significant increase in circadian plasticity. The orange line marks the median pre-dawn activity of the *D. sechellia* parental strain (07).

1438

1439

1440

1441

1442

1443

c, Mean normalized activity of the indicated genotypes under a 12:12 h LD cycle. Dashed boxes highlight the pre-dawn area used to quantify morning anticipation. Sample sizes as follows:  $w^{1118}$  (78), 28/ $w^{1118}$  (22), 28/*CCHa1* (4), 28/*Clk* (64), 28/*cwo* (20), 28/*cyc* (56), 28/*Cry* (66), 28/*Fer* (5), 28/*Hr38* (43), 28/*IITP* (25), 28/*Jet* (22), 28/*Pdf* (21), 28/*PDP1* (14), 28/*scro* (38), 28/*vri* (33), 28 (36).

1444

1445

1446

1447

1448

1449

d, Mean normalized pre-dawn activity for the genotypes in C. Asterisks indicate significant differences: \* =  $p < 0.05$  and \*\*\* =  $p < 0.001$  (Wilcoxon tests comparing each test hybrid to the control hybrid strain (28/ $w^{1118}$ ) with Bonferroni correction). The orange line marks the median pre-dawn activity of the *D. sechellia* parental strain (28).

1450

1451

1452

1453

1454

e, Mean normalized activity of the indicated hemizygous *D. melanogaster* genotypes that displayed an effect in a hybrid background under a 12:12 h LD cycle. Dashed boxes highlight the pre-dawn area used to quantify morning anticipation. (07 or 28) under a 12h LD cycle. Plots depict average activity of the last 4 days of a 7 day recording period. Dashed boxes highlight the pre-dawn period, 3 h before lights-on. Sample sizes as follows:  $w^{1118}$  (78), *Clk*/ $w^{1118}$  (25), *cyc*/ $w^{1118}$  (31), *Cry*/ $w^{1118}$  (32), *Hr38*/ $w^{1118}$  (25), *vri*/ $w^{1118}$  (46).

1455

1456

1457

1458

1459

1460

1461

f, Mean normalized pre-dawn activity for the genotypes in e. Asterisks indicate significant differences: \* =  $p < 0.05$  (Wilcoxon tests comparing each test hemizygote to the control strain ( $w^{1118}$ ) with Bonferroni correction). Red asterisks denote a significant increase in pre-dawn activity.

1462

1463

1464

1465

1466

g, Summary of the overlapping hits from each of the above genotypes. *A priori*, we considered the strongest candidates to display a reduction in morning anticipation in *Dsec07* and *Dsec28* hybrids, but not in  $w^{1118}$  hemizygotes. See Extended Data Fig. 3g legend for notes on the *Clk*/ $w^{1118}$  mutant phenotype.

1467

1468

1469

1470

1471

1472

**Extended Data Fig. 5. The predicted Pdf protein sequence is highly conserved between *D. melanogaster*, *D. sechellia* and *D. simulans*.**

1473

1474

1475

1476

Alignment of the predicted Pdf protein sequence of 10 *D. melanogaster*, 6 *D. sechellia* and 5 *D. simulans* strains. Amino acid residues are coloured by similarity, periods indicate conserved amino acid residues and letters indicate variable

1477 residues. No fixed differences are observed between species. The consensus  
1478 sequence is displayed at the bottom.

1479

1480 **Extended Data Fig. 6. Validation of differential *Pdf* transcript depletion by**  
1481 **smFISH.**

1482 Left: representative smFISH images for one genetic control (*UAS-Pdf<sup>RNAi/+</sup>*),  
1483 *DmelPdf-Gal4/UAS-Pdf<sup>RNAi</sup>* and *DsecPdf-Gal4/UAS-Pdf<sup>RNAi</sup>* strains with RNA spots  
1484 identified by RS-FISH. Right: RNA spot quantifications. N = 5 for each genotype.

1485

1486 **Extended Data Fig. 7. Pdf immunofluorescence in the I-LNVs of *D.***  
1487 ***melanogaster* and *D. sechellia* during the evening peak.**

1488 **a**, Left: representative images of Pdf immunofluorescence in the I-LNV soma for  
1489 the CS and 07 strains under 12:12 h LD at one time point (6 h). Right:  
1490 quantifications of Pdf signals at 5 time points spanning the evening activity  
1491 peak period.

1492 **b**, Quantifications of Pdf signals at 5 time points spanning the evening activity  
1493 peak period in the I-LNV soma for the CS and 07 strains under 16:8 h LD.

1494

1495 **Extended Data Fig. 8. Correlations of minor allele frequency and latitude in**  
1496 ***D. melanogaster* populations for control neuropeptide genes.**

1497 Each plot depicts the correlation between minor allele frequency and latitude for  
1498 the putative 5'-regulatory region (~2.4 kb upstream of the start codon) for the  
1499 indicated neuropeptide genes. For reference, the analysis for the *Pdf* 5'-regulatory  
1500 region (from Fig. 5c) is shown on the first plot. Values for Spearman's rho and  
1501 Bonferroni corrected p-values are listed above each plot.

1502

1503 **Extended Data Fig. 9. Qualitatively similar circadian plasticity and pre-dawn**  
1504 **activity in two Canton-S strains.**

1505 **a**, Mean normalized activity of two *Canton-S* (CS and CS<sup>W</sup>) strains collected  
1506 under a 16:8 h LD cycle. Plots depict average activity of the last 4 days of a  
1507 7-day extended photoperiod, following 7 days of 12:12 h LD. Vertical dashed  
1508 lines indicate the average timing of the evening peak for each strain. Sample  
1509 sizes as follows: CS (18), CS<sup>W</sup> (16).

1510 **b**, Evening peak time for the flies depicted in **a** is shown for each strain. No  
1511 significant difference was observed between strains (Wilcoxon test).

1512 **c**, Mean normalized activity of two *Canton-S* strains (CS and CS<sup>W</sup>) under a 12:12  
1513 h LD cycle. Plots depict average activity of the last 4 days of a 7-day  
1514 recording period. Dashed boxes highlight the pre-dawn period, 3 h before  
1515 lights-on. Sample sizes as follows: CS (29), CS<sup>W</sup> (42).

1516 **d**, The average activity for flies shown in **c** within the previously indicated pre-  
1517 dawn period, mean normalized pre-dawn activity, is shown for each strain.  
1518 Asterisks indicate significant differences: \*\* = p < 0.01 (Wilcoxon test).

1519

1520 **Supplementary Tables**

1521

1522 **Supplementary Table 1. *Drosophila* strains.**

Stock Name	Genotype	Species	Reference	Hybridized
Canton-S (CS)	<i>wt</i>	<i>D. melanogaster</i>	RRID:BDSC_64349	N/A
Oregon-R (OR)	<i>wt</i>	<i>D. melanogaster</i>	RRID:BDSC_2376	N/A
LZV L72	<i>wt</i>	<i>D. melanogaster</i>	<sup>94</sup>	N/A
LZV L76	<i>wt</i>	<i>D. melanogaster</i>	<sup>94</sup>	N/A
LZV A10	<i>wt</i>	<i>D. melanogaster</i>	<sup>94</sup>	N/A
MD221	<i>wt</i>	<i>D. simulans</i>	<sup>94</sup>	N/A
MD242	<i>wt</i>	<i>D. simulans</i>	<sup>94</sup>	N/A
LZV L47	<i>wt</i>	<i>D. simulans</i>	<sup>94</sup>	N/A
<i>Dsim04</i>	<i>wt</i>	<i>D. simulans</i>	DSSC 14021-0251.004	N/A
<i>Dsim196</i>	<i>wt</i>	<i>D. simulans</i>	DSSC 14021-0251.196	N/A
<i>Dsec07</i>	<i>wt</i>	<i>D. sechellia</i>	DSSC 14021-0248.07	N/A
<i>Dsec28</i>	<i>wt</i>	<i>D. sechellia</i>	DSSC 14021-0248.28	N/A
<i>Dsec19</i>	<i>wt</i>	<i>D. sechellia</i>	DSSC 14021-0248.19	N/A
<i>Dsec21</i>	<i>wt</i>	<i>D. sechellia</i>	DSSC 14021-0248.21	N/A
<i>Dsec30</i>	<i>wt</i>	<i>D. sechellia</i>	DSSC 14021-0248.30	N/A
<i>Dsec31</i>	<i>wt</i>	<i>D. sechellia</i>	DSSC 14021-0248.31	N/A
<i>Dmau90</i>	<i>wt</i>	<i>D. mauritiana</i>	DSSC 14021-0241.90	N/A
<i>Dmau91</i>	<i>wt</i>	<i>D. mauritiana</i>	DSSC 14021-0241.91	N/A
<i>w<sup>1118</sup></i>	<i>w<sup>1118</sup></i>	<i>D. melanogaster</i>	RRID:BDSC_3605	07 and 28
Würzburg Canton-S (CS <sup>W</sup> )	<i>wt</i>	<i>D. melanogaster</i>	Gift of C. Förster	07 and 28
<i>Pdf<sup>01</sup></i>	<i>Pdf<sup>01</sup></i> (in CS <sup>W</sup> background)	<i>D. melanogaster</i>	Gift of C. Förster	07 and 28
<i>Hr38</i>	<i>w<sup>*</sup>; dpy ov1 bw1 Hr3856/CyO, P{GAL4-twi.G}2.2, P{UAS-2xEGFP}AH2.2</i>	<i>D. melanogaster</i>	RRID:BDSC_76590	07 and 28
<i>Clk</i>	<i>Clk<sup>Jrk</sup></i>	<i>D. melanogaster</i>	RRID:BDSC_80927	07 and 28
<i>PDP1</i>	<i>w<sup>1118</sup>; Pdp13135/TM3, Sb1</i>	<i>D. melanogaster</i>	RRID:BDSC_80925	07 and 28
<i>cyc</i>	<i>cyc<sup>01</sup></i>	<i>D. melanogaster</i>	RRID:BDSC_80929	07 and 28
<i>scro</i>	<i>scro<sup>Z211</sup></i>	<i>D. melanogaster</i>	RRID:BDSC_81875	07 and 28
<i>cwo</i>	<i>w<sup>1118</sup>; PBac{RB}cwoe04207/TM 6B, Tb1</i>	<i>D. melanogaster</i>	RRID:BDSC_85593	07 and 28
<i>Cry</i>	<i>w<sup>1118</sup>; ss cryb</i>	<i>D. melanogaster</i>	RRID:BDSC_80921	07 and 28
<i>Df(vri)</i>	<i>w<sup>1118</sup>; Df(2L)Exel6011, P{XP-U}Exel6011/CyO</i>	<i>D. melanogaster</i>	RRID:BDSC_7497	07 and 28
<i>Rh7</i>	<i>y1; Rh70</i>	<i>D. melanogaster</i>	RRID:BDSC_83716	07, not 28
<i>Jet<sup>c</sup></i>	<i>y1 w<sup>*</sup>; jetc</i>	<i>D. melanogaster</i>	RRID:BDSC_27641	No
<i>Jer</i>	<i>y1 w<sup>*</sup>; jetr</i>	<i>D. melanogaster</i>	RRID:BDSC_27641	No

<i>Df(Jet)</i>	<i>w</i> <sup>1118</sup> ; <i>Df(2L)ED7853, P{3'.RS5+3.3}ED7853/S M6a</i>	<i>D. melanogaster</i>	RRID:BDSC_24124	07 and 28
<i>CCHa1</i>	<i>y[1] w[*]; Mi{y[+mDint2]=MIC}CCHa 11[MI09190]</i>	<i>D. melanogaster</i>	RRID:BDSC_51261	07, poorly with 28
<i>ITP</i>	<i>w</i> <sup>1118</sup> ; <i>PBac{w[+mC]=RB}ITP[e0 2889]/CyO</i>	<i>D. melanogaster</i>	RRID:BDSC_85570	07 and 28
<i>tim</i>	<i>y[1] w[*]; tim[01]</i>	<i>D. melanogaster</i>	RRID:BDSC_80922	No
<i>Df(tim)</i>	<i>y1 w*</i> ; <i>Df(2L)drm-P2, P{lacW}ND-PDSWk10101/SM6b</i>	<i>D. melanogaster</i>	RRID:BDSC_6507	No
<i>sr</i>	<i>y</i> <sup>1</sup> <i>w</i> <sup>*</sup> ; <i>P{neoFRT}82Bsr<sup>155</sup>/TM3, Sb<sup>1</sup></i>	<i>D. melanogaster</i>	RRID:BDSC_36535	No
<i>Fer2</i>	<i>w</i> <sup>1118</sup> ; <i>PBac{RB}Fer2e03248</i>	<i>D. melanogaster</i>	RRID:BDSC_86028	07, poorly with 28
<i>DmelPdf-Gal4</i>	<i>y1 w67c23;;P{Dmel-Pdf-Gal4}attP2</i>	<i>D. melanogaster</i>	This work	N/A
<i>DsecPdf-Gal4</i>	<i>y1 w67c23;;P{Dsec-Pdf-Gal4}attP2</i>	<i>D. melanogaster</i>	This work	N/A
<i>DmelPdf-CD4:tdGFP</i>	<i>y1 w67c23;;P{DmelPdf-CD4:tdGFP}attP2</i>	<i>D. melanogaster</i>	This work	N/A
<i>DsecPdf-CD4:tdGFP</i>	<i>y1 w67c23;;P{DsecPdf-CD4:tdGFP}attP2</i>	<i>D. melanogaster</i>	This work	N/A
<i>UAS-Pdf<sup>RNAi</sup></i>	<i>y[1] v[1]; P{y[+t7.7] v[+t1.8]=TRiP.JF01820}att P2</i>	<i>D. melanogaster</i>	RRID:BDSC_25802	N/A

1523

1524

### Supplementary Table 2. Antibodies.

Antibody	Dilution	Reference/source	Identifier
Mouse anti-Pdf C7	1:400	Developmental Studies Hybridoma Bank	AB_760350 AB_2315084
Rabbit anti-GFP	1:1000	Invitrogen	Cat #A-11122
Rat anti-DNCadherin (DN-Ex#8) (Cadherin-N)	1:25	Developmental Studies Hybridoma Bank	AB_528121
Goat Alexa488 anti-mouse	1:100	Molecular Probes, Jackson ImmunoResearch	AB_2338840
Goat Alexa488 anti-rabbit	1:100	Molecular Probes, Jackson ImmunoResearch	AB_2338049
Donkey Cy5 anti-rat	1:200	Molecular Probes, Jackson ImmunoResearch	AB_2340672

1525

1526

### Supplementary Table 3. Oligonucleotides.

Purpose	PCR product	Sequences (5'-3') sense / antisense
<i>Pdf</i> gene sequencing	CDS + 5'-regulatory region I	catttctctcgacgcacca / ccaactgccgagctagctat
	5'-regulatory region II	aaactaatagctagctcggcag / aatgtggctgcatggaag
	5'-regulatory region III	aaacattgacccaactccgc / gtttcatcctaccagcgc
Entry clone for <i>Pdf</i> 5'-regulatory region Gateway cloning	5' regulatory region (~2.4 kb upstream of start codon)	ggggacaactttgtacaaaaaagttggcaccggccacatagtgcccagta / ggggacaactttgtacagaagaaagttggcaatagtcaggagctggaagg

1527

**Figure 1**

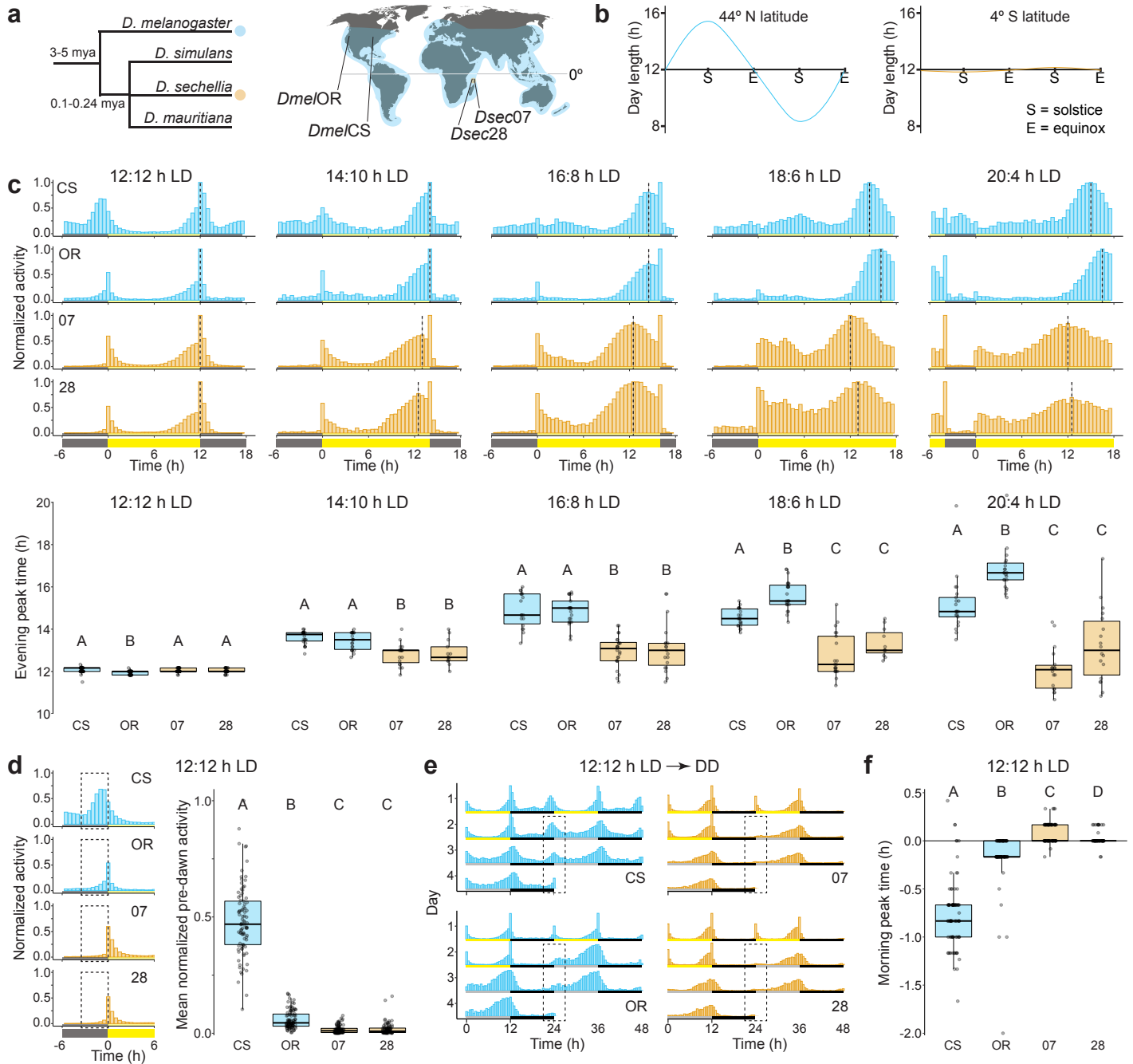


**Figure 2**

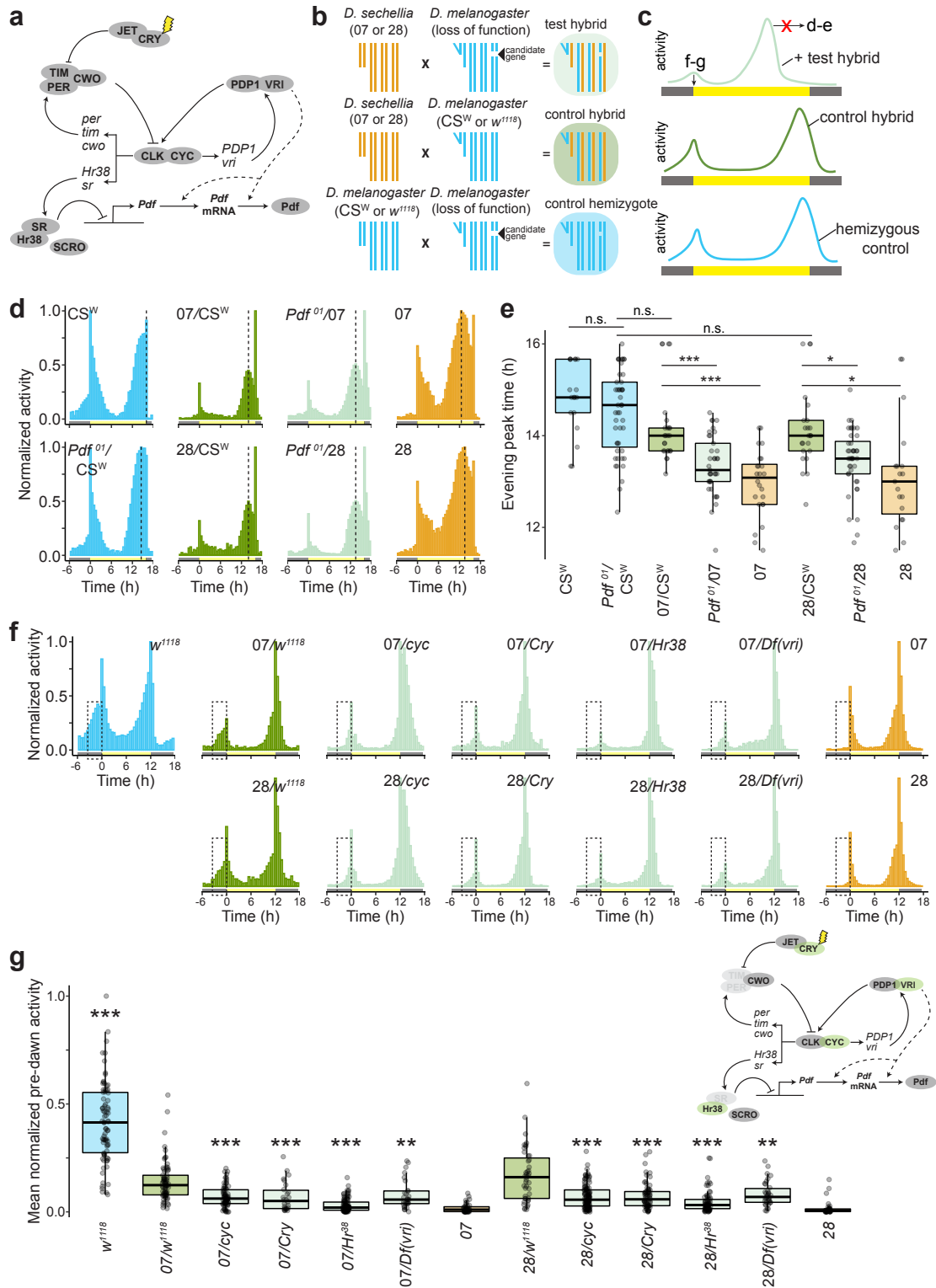


**Figure 3**

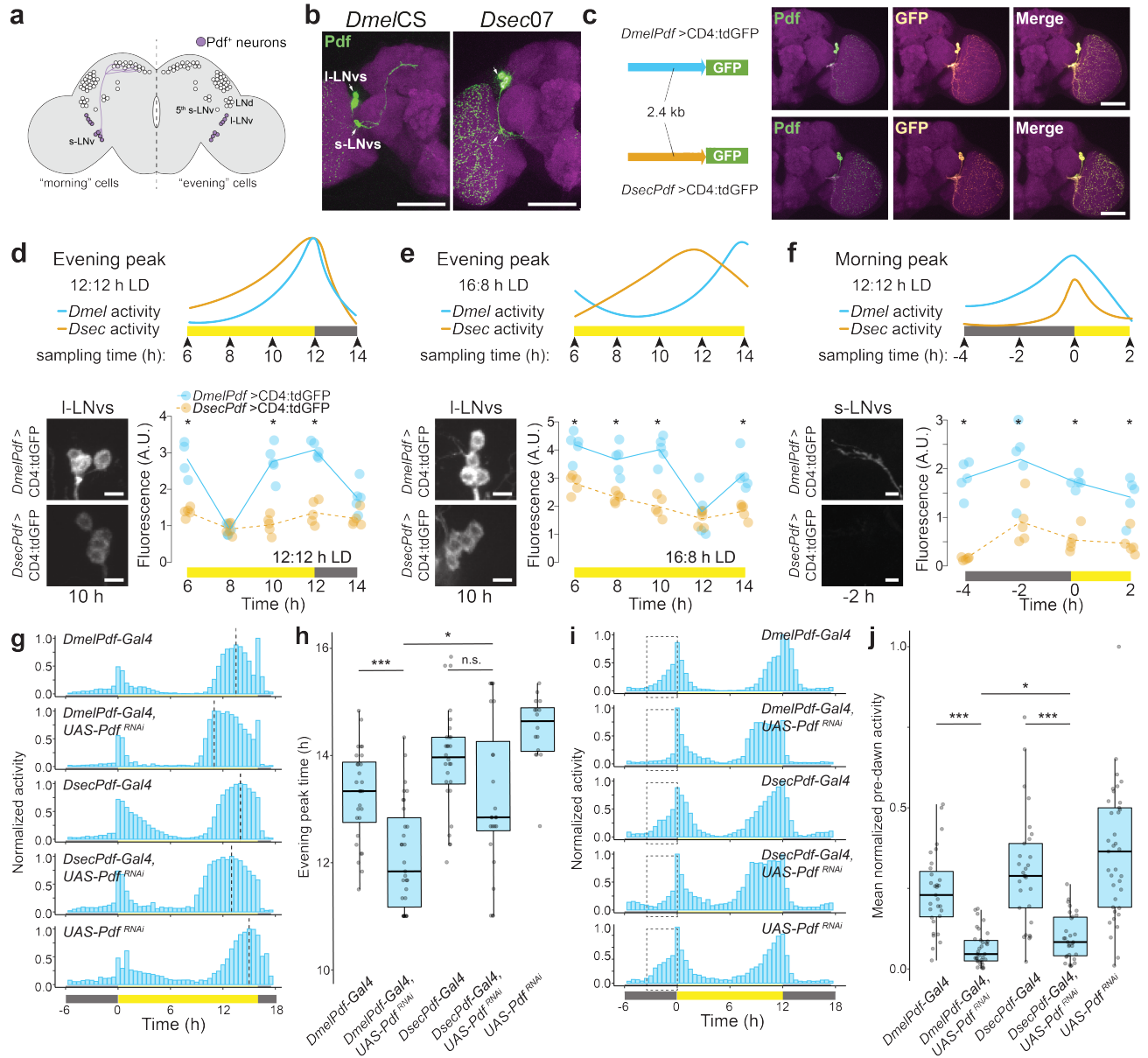


## Figure 4

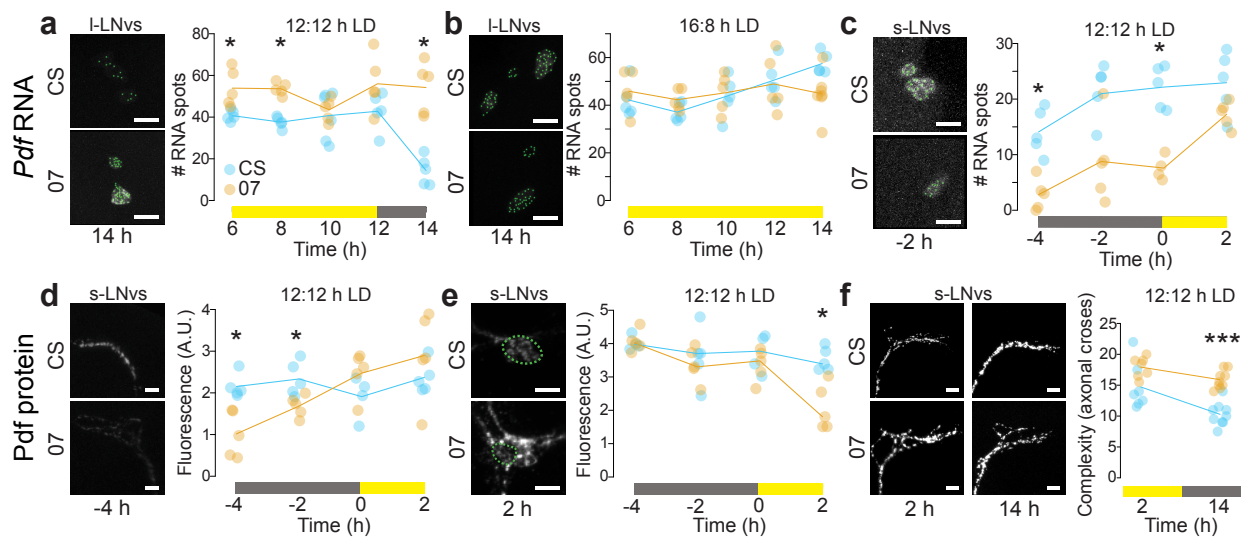
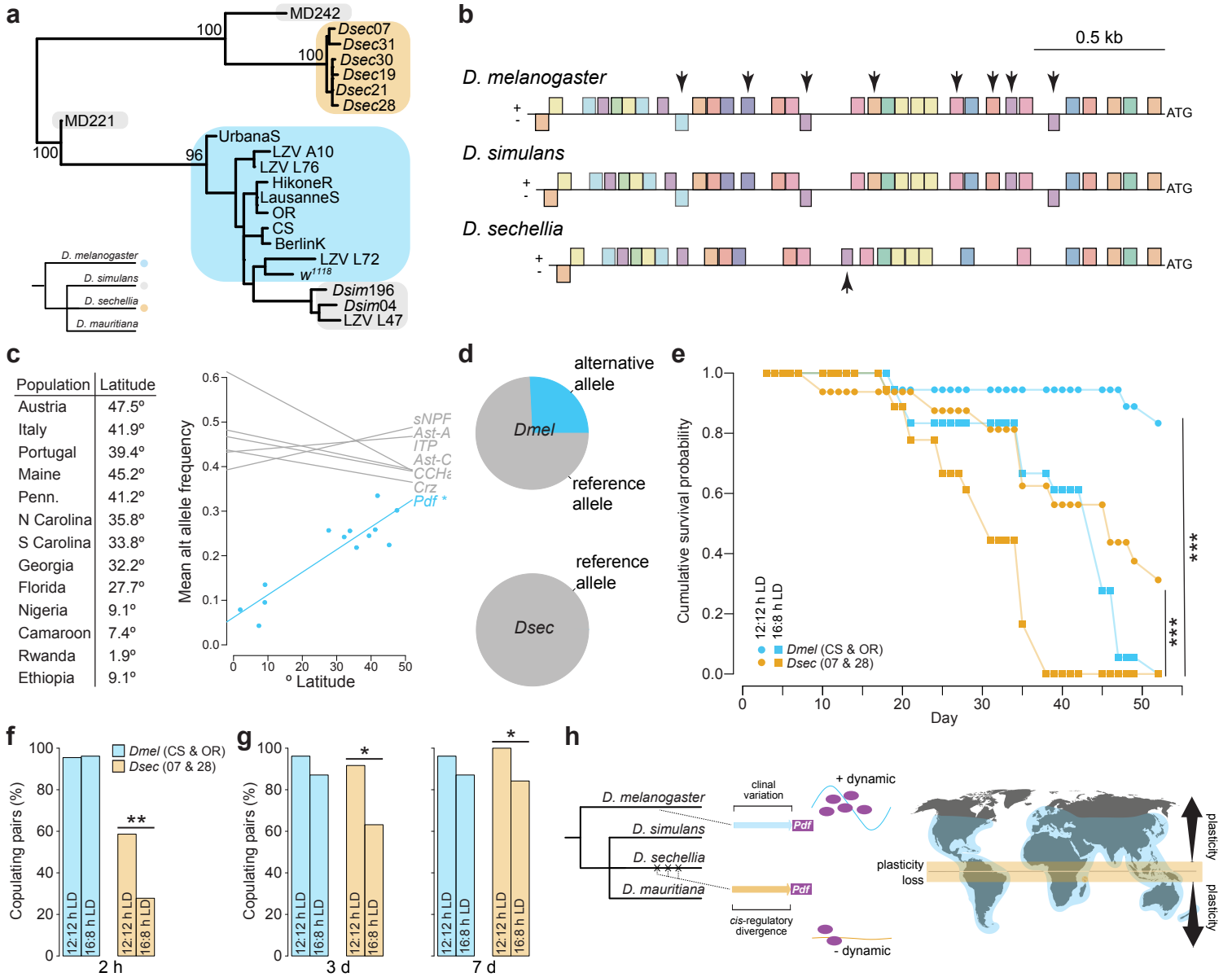
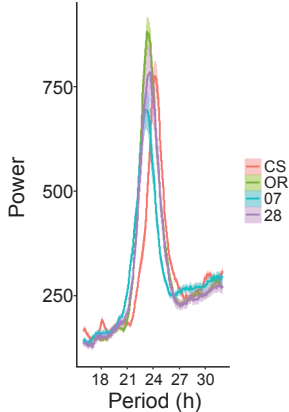


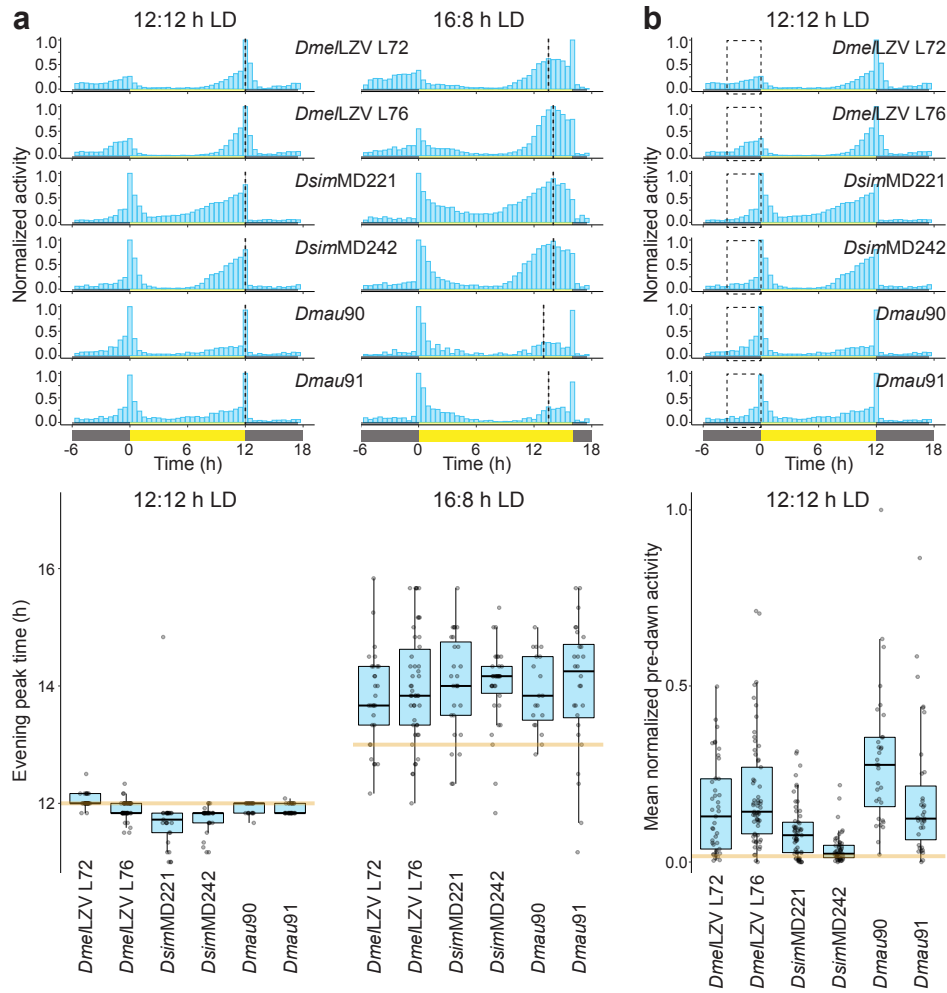
**Figure 5**



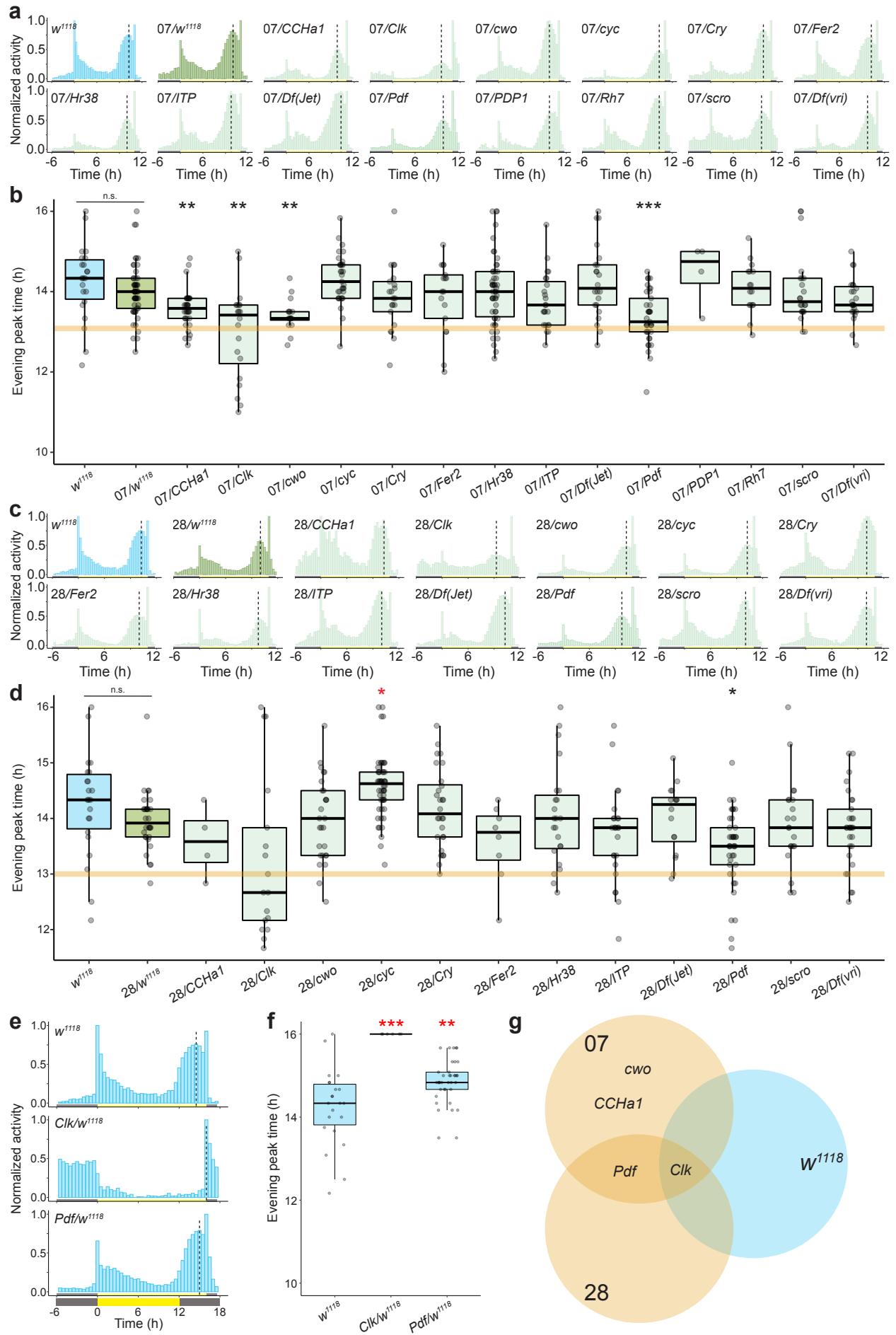
ED Figure 1



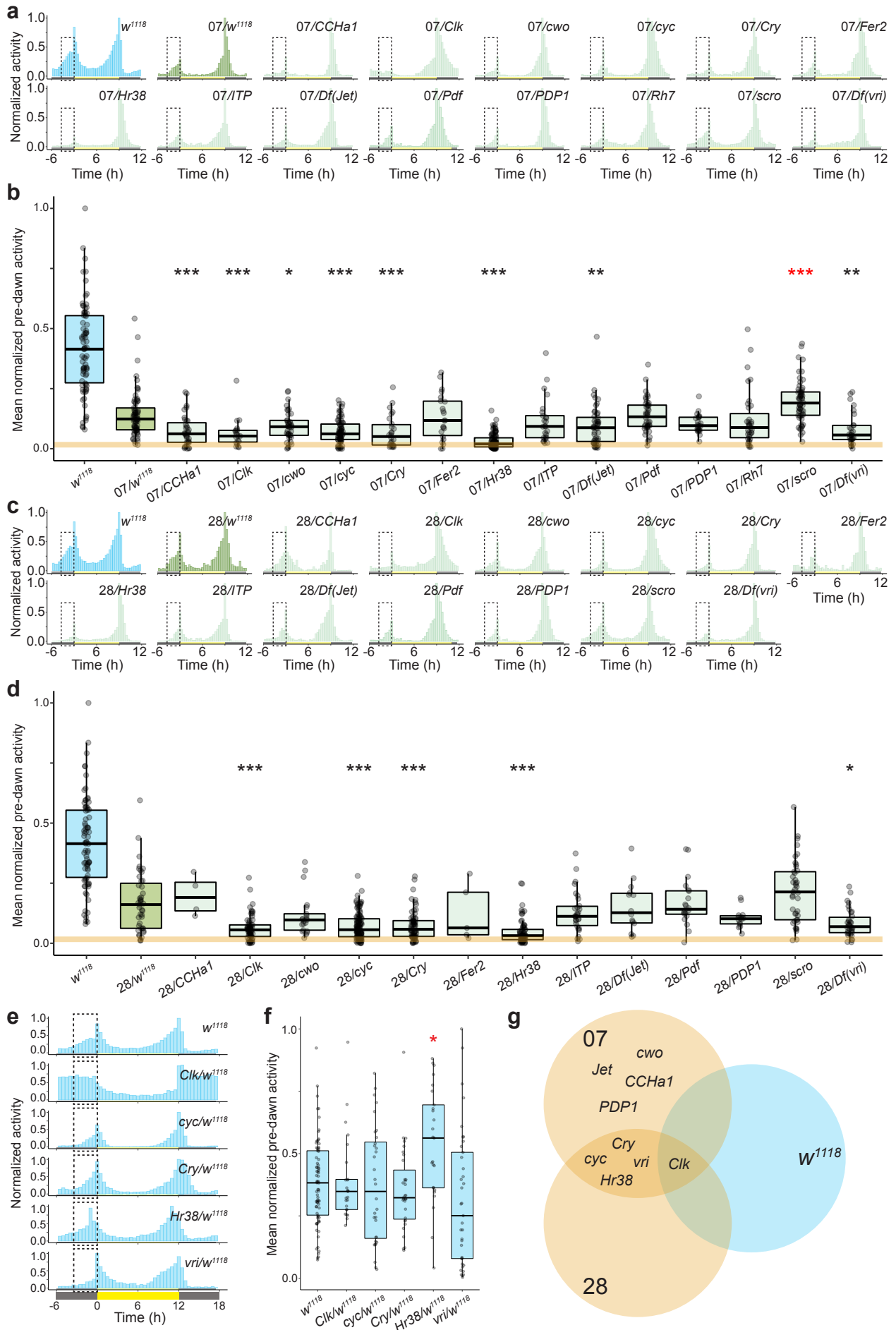
# ED Figure 2



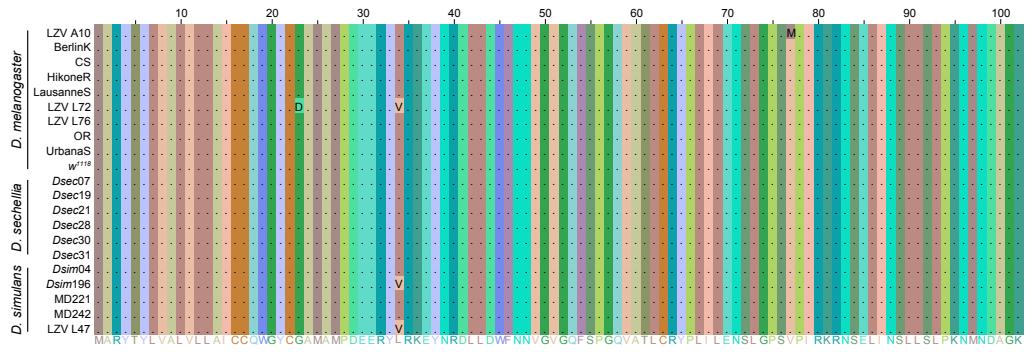
# ED Figure 3



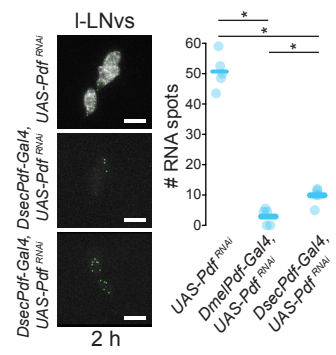
# ED Figure 4



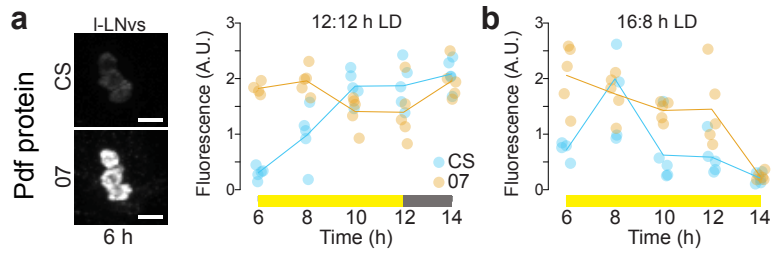
# ED Figure 5



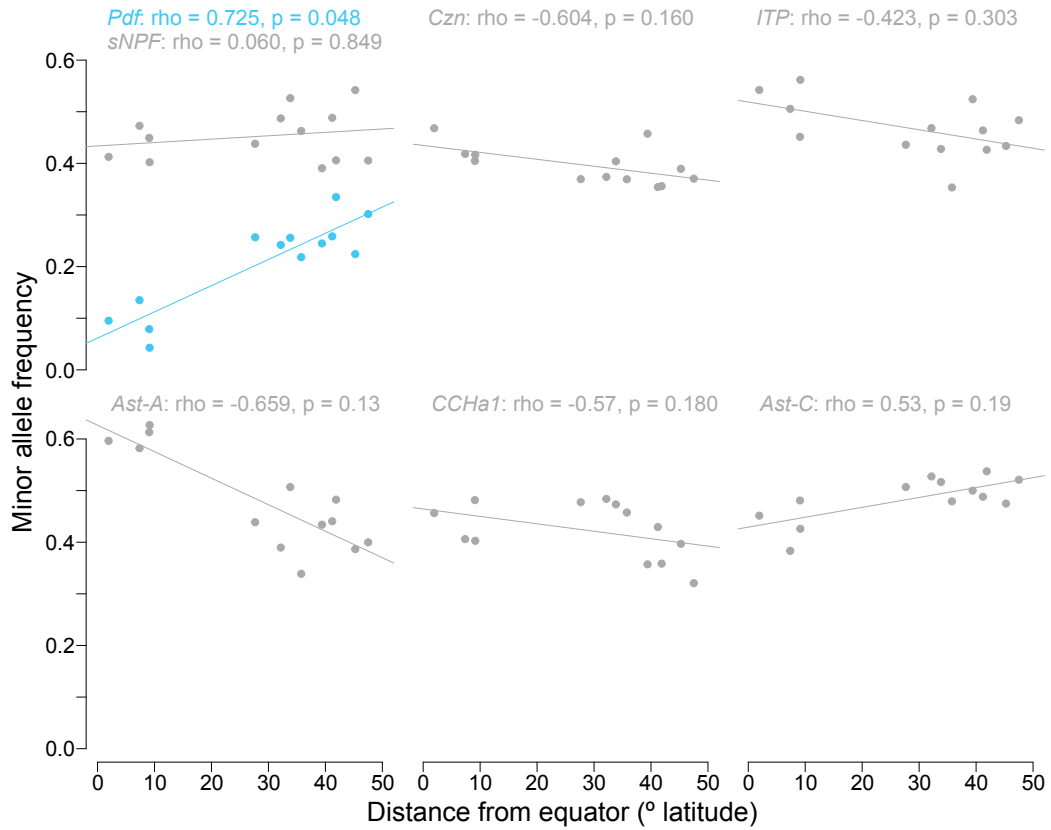
# ED Figure 6



# ED Figure 7



# ED Figure 8



# ED Figure 9

